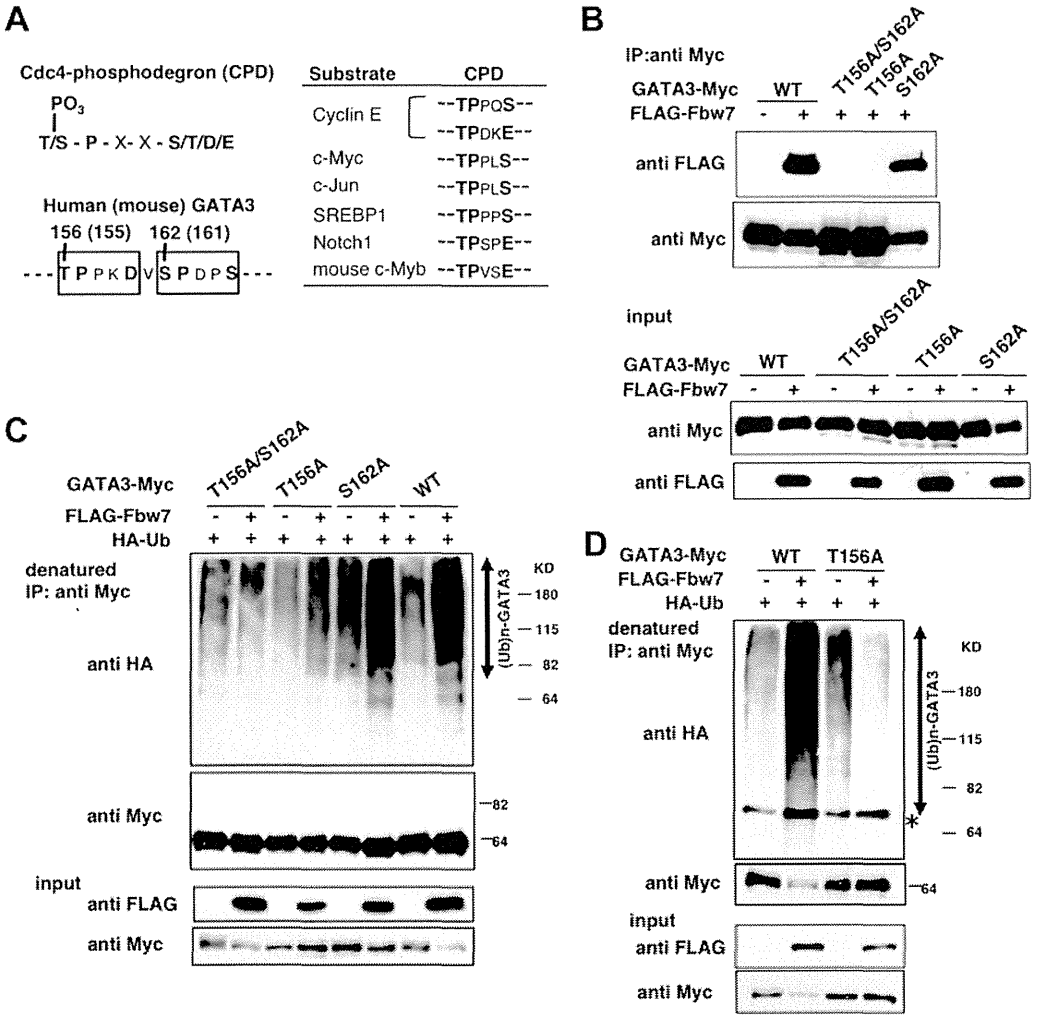

FIG 5 Fbw7 promotes ubiquitylation of GATA3 in a Thr-156-dependent manner. (A) Sequence alignment of known Fbw7 substrates containing the Cdc4 phosphodegron (CPD) consensus sequence for recognition by Fbw7. Conserved residues within the CPD are shown in bold. Two putative CPD sites (open box) in human and mouse GATA3 are indicated. Numbered residues indicate putative phosphorylation sites. (B) Fbw7 binding to GATA3 is dependent on Thr-156 in GATA3 *in vivo*. HEK293 cells were transfected with Myc-tagged wild-type (WT) or mutant GATA3 along with FLAG-Fbw7, as indicated, and incubated with 20 μM MG132 for 5 h. Cell lysates were immunoprecipitated (IP) with antibodies against Myc, followed by immunoblotting for FLAG and Myc (top panels). Immunoblot analysis of input from each transfection confirmed expression levels of WT GATA3, mutant GATA3, and Fbw7 (bottom panels). (C) HEK293 cells were transfected with Myc-tagged WT or mutant GATA3, FLAG-Fbw7, and HA-ubiquitin as indicated. Cells were incubated with 20 μM MG132 for 5 h, lysed, and denatured with sample buffer containing SDS and 2-mercaptoethanol to dissociate proteins associated with GATA3. Myc-tagged GATA3 was immunoprecipitated and analyzed by immunoblotting with the indicated antibodies (top panels). Whole-cell extracts (input) were subjected to immunoblotting to confirm protein expression (bottom panels). (D) The same experiment as described in panel A was performed in HeLa cells.

Coexpression of Fbw7 significantly facilitated the degradation of WT GATA3 (Fig. 6 left). In contrast, the T156A mutant was relatively stable compared with WT GATA3 in the absence of Fbw7, and its level did not change with Fbw7 (Fig. 6). These results suggest that modification of GATA3 on Thr-156 is one of the key events for recognition by SCF^{Fbw7}, which mediates GATA3 ubiquitylation and degradation. Moreover, owing to degradation of WT GATA3 by coexpressed Fbw7, protein levels of WT GATA3 in the presence of HA-Fbw7 were significantly reduced in comparison with levels in the absence of HA-Fbw7, even at the first measurement of this assay (0.1 h).

CDK2 phosphorylates Thr-156 in GATA3. We speculated that like other substrates of Fbw7, regulation of GATA3 by Fbw7 would be mediated by phosphorylation of Thr-156 in the CPD. To evaluate whether Thr-156 of GATA3 was phosphorylated in intact cells, a phospho-specific antibody (anti-P-T156-GATA3) that recognizes phosphorylated Thr-156 was prepared. Myc-tagged WT GATA3 expressed in HEK293 cells treated with both phosphatase and proteasome inhibitors was detected by the anti-P-T156-GATA3 antibody, but no signal was detected using the GATA3 T156A mutant (Fig. 7A). These data suggest that GATA3 Thr-156 is phosphorylated *in vivo*.

Fbw7-mediated degradation of substrate is often triggered by the activation of GSK3 (1, 4, 5, 30, 31). GSK3 phosphorylates Ser and Thr residues, after an initial "priming phosphorylation" of a Ser or Thr located four amino acids C-terminal to the site of GSK phosphorylation (32). If Asp and Glu can be considered to mimic this priming phosphorylation, the residues surrounding Thr-156

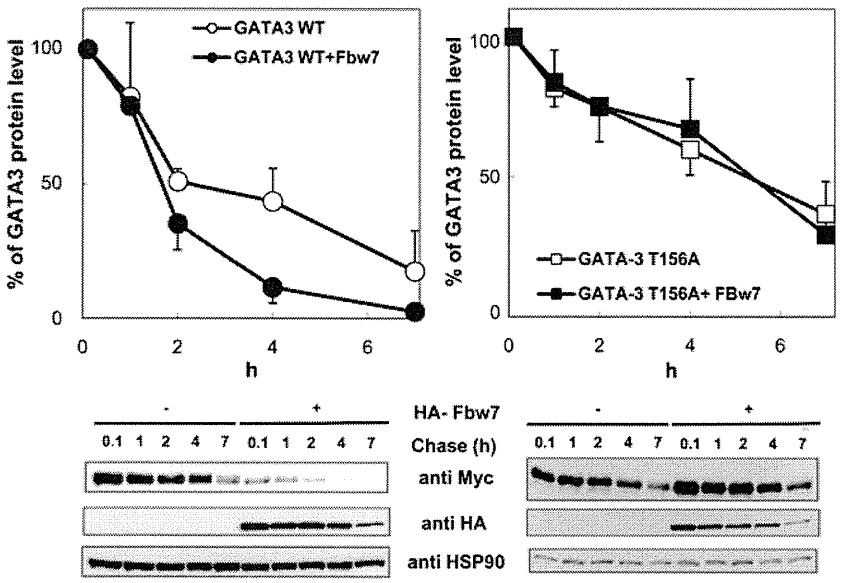

FIG 6 Fbw7 promotes degradation of GATA3 in a Thr-156-dependent manner. HeLa cells were transfected with Myc-tagged WT (left) or T156A GATA3 (right) in the absence or presence of HA-Fbw7 and treated with 12.5 μg/ml cycloheximide to inhibit protein synthesis for the indicated times. GATA3 levels were analyzed at various time points by immunoblotting (bottom panels). The percentage of GATA3 at each time point was quantitated by image analysis and normalized against HSP90 (top panels). GATA3 protein levels were calculated as the means ± SDs from three independent experiments. Immunoblots show data from one representative experiment.

in GATA3 can be classified as a GSK3 phosphorylation consensus motif (Fig. 5A, left). To examine whether GSK3 phosphorylates Thr-156 of GATA3 *in vitro*, we prepared two types of synthetic peptides (amino acids [aa] 150 to 161 of GATA3) for the WT and the Thr-156 mutant sequence in which Thr was replaced with Ala (T156A). Unexpectedly, there was no detectable incorporation of ^{32}P in the WT or T156A peptide, indicating that GSK3 does not phosphorylate either peptide (Fig. 7B, top). We examined other Ser/Thr kinases and found that cyclin E/CDK2 and cyclin A/CDK2, but not cyclin B1/CDK1, specifically phosphorylated WT GATA3 peptide (Fig. 7B, top). Their kinase activity was confirmed using the S11 peptide, which is a confirmed substrate for CDK1, CDK2, and CDK4/CDK 6 (Fig. 7B, bottom) (22).

To further confirm the specific phosphorylation on Thr-156, GST fusion recombinant GATA3 proteins, WT and T156A mutant, were examined as substrates. Reduced CDK2-mediated phosphorylation of the T156A mutant compared with WT GATA3 was confirmed by immunoblotting with anti-phospho-Thr and anti-P-T156-GATA3 antibodies (Fig. 7C and D). A previous study reported that GATA3 is also phosphorylated by p38 MAPK (33, 34). Consistent with this report, p38 strongly phosphorylated both recombinant GATA3 proteins (Fig. 7C) although it did not exhibit kinase activity toward Thr-156 in GATA3 (Fig. 7B, top, and D).

Physiological CDK2, which is activated during G_2/M phase, works on Thr-156 of GATA3 and regulates its stability. We further investigated physiological effects on GATA3 of CDK2. Reduction of CDK2 by siRNA inhibited phosphorylation on Thr-156, providing evidence that CDK2 is involved in CPD phosphorylation of GATA3 *in vivo* (Fig. 8A). To verify the requirement of phosphorylation of GATA3 for binding to Fbw7, we tested the binding ability of phosphorylated GATA3 to Fbw7 *in vitro*. WT GATA3 phosphorylated by CDK2 was able to bind Fbw7, while the T156A GATA3 mutant did not, regardless of the phosphorylating kinase (Fig. 8B). These results suggest that CDK2-mediated phosphorylation of Thr-156 is essential for binding of GATA3 to Fbw7.

Cyclin E/CDK2 plays a critical role in the G_1/S-phase transition (35). Cyclin A then replaces cyclin E to associate with CDK2, and this complex subsequently functions in S-phase progression and G_2/M transition (36). We conducted an *in vitro* phosphorylation assay using cell lysates prepared from G_1/S or G_2/M synchronized or nonsynchronized HeLa cells as the kinase source. Recombinant GATA3 was phosphorylated only in the presence of G_2/M lysate even though both cyclin A and cyclin E protein levels in the lysate were decreased (Fig. 8C). To verify the responsible kinase in the G_2/M lysate, we tested the effects of a CDK2 inhibitor (CVT313) and competitor (p27) on kinase activity. Both p27 and CVT313 inhibited the kinase activity on Thr-156 in a dose-dependent manner (Fig. 8D).

Phosphorylation at Thr-156 in GATA3 is executed in HUT78 cells during G_2/M phase and in thymocytes of mice. Cell cycle-dependent phosphorylation of CPD in endogenous GATA3 was also confirmed in the HUT78 cell line, which is a T-cell lymphoma line. Phosphorylated Thr-156 was detected in G_2/M arrested cells but not in nonsynchronized cells, which contained a G_2/M population of only approximately 15% (Fig. 8E). We further investigated the property of Thr-156-phosphorylated GATA3. MG132 treatment resulted in an accumulation of Thr-156-phosphorylated GATA3 in G_2/M (Fig. 8F). This implies that phosphorylation of GATA3 at Thr-156 induces its proteasome-dependent degradation during G_2/M. These results suggest that cyclin A/CDK2 regulates GATA3 stability through the phosphorylation of the CPD during G_2/M phase in cultured cells. GATA3 Thr-156 phosphorylation was also detected in mouse thymocytes (Fig. 8G). Furthermore, ICC analysis using anti-phospho-Thr-156 antibody

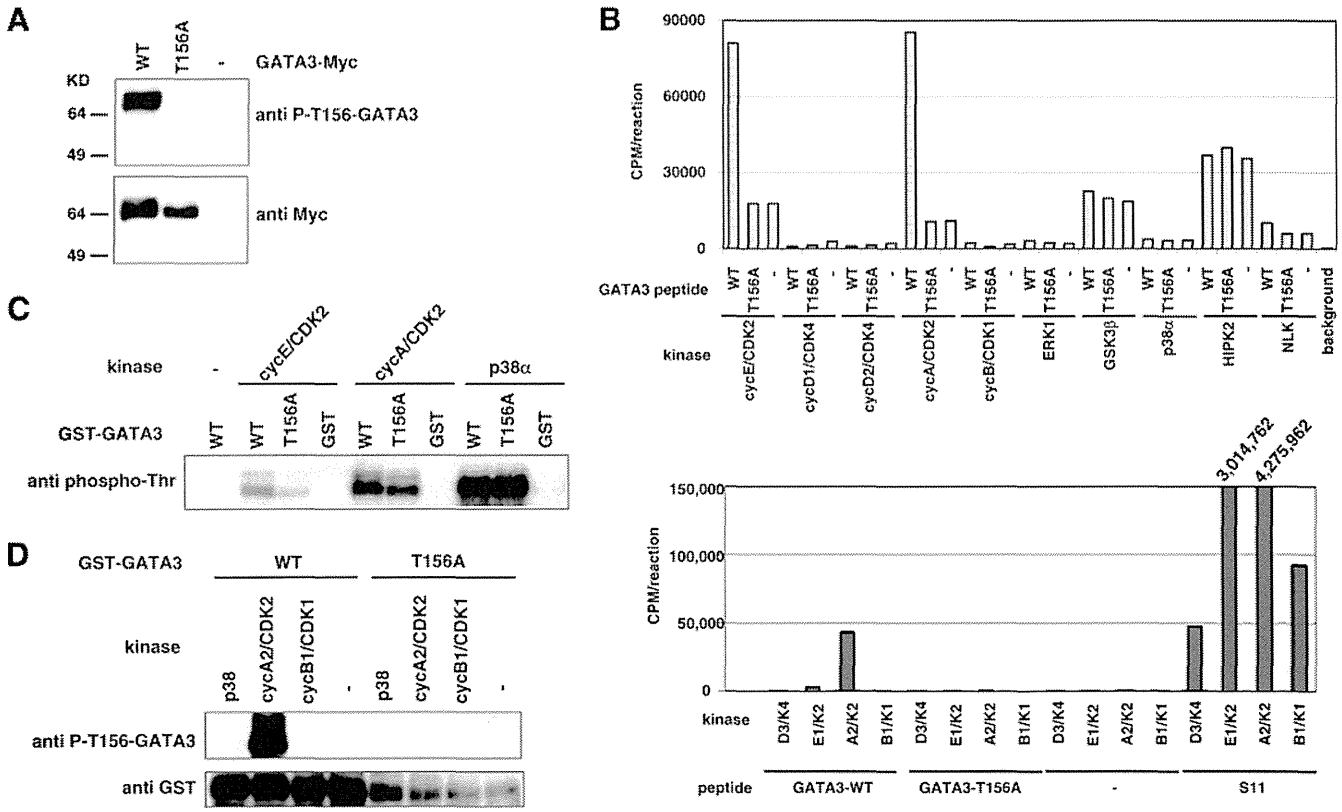

FIG 7 Thr-156 of GATA3 is phosphorylated by CDK2. (A) Transiently expressed GATA3 is phosphorylated at Thr-156 in HEK293 cells. HEK293 cells were transfected with WT or T156A GATA3 and treated with 20 μM MG132 and 20 nM okadaic acid for 5 h to inhibit proteolysis and dephosphorylation of GATA3. Cell lysates were prepared with lysis buffer containing phosphatase inhibitors and protease inhibitors and subjected to immunoblot analysis using phospho-T156-GATA3 or Myc antibodies. (B) CDK2 phosphorylates GATA3 peptide in a Thr-156-dependent manner *in vitro*. A synthetic peptide corresponding to aa 150 to 161 of WT or T156A GATA3 was incubated with [γ-^{32}P]ATP and the indicated kinases at 30°C for 30 min (top panel). S11 peptide (KAPLTPKKAK) is efficiently phosphorylated by various CDKs (22). To confirm the activities of the CDKs used in our experiments, we performed *in vitro* kinase assays using the S11 peptide as a positive control. Wild-type or T156A synthetic GATA3 peptide or S11 peptide was incubated with [γ-^{32}P]ATP along with the indicated CDKs at 30°C for 30 min (bottom panel). The peptides were trapped on P81 papers and monitored for radioactivity using a liquid scintillation counter. (C and D) Recombinant GATA3 is phosphorylated at Thr-156 by CDK2 *in vitro*. WT or T156A GST-fused GATA3 was expressed in *E. coli* and affinity purified using glutathione-Sepharose 4B. GST alone was prepared in parallel as a control. The proteins were incubated with the kinases as indicated in reaction buffer at 30°C for 30 min. Reaction products were subjected to immunoblot analysis with the indicated antibodies.

detected phosphorylated Thr-156 in GATA3 in the DN subset of thymocytes (data not shown). We found that phosphorylation of Thr-156 in GATA3 in DP subsets was observed at an equal level relative to that in DN subsets (DN/DP, 1:1.16) (data not shown). Because GATA3 accumulates in the DN but not in the DP subset in Lck-Cre/*Fbw7*$^{flox/flox}$ mice (Fig. 3A), Thr-156 phosphorylation of GATA3 may participate in Fbw7-mediated degradation of GATA3 in the DN subset. In contrast, an unknown mechanism that suppresses Fbw7-mediated degradation of GATA3 may be present in the DP lineage, while Thr-156 phosphorylation of GATA3 was observed.

DISCUSSION

Half of GATA3-overexpressing CD2-GATA3 Tg mice developed thymic lymphoblastoid tumors (6). This may be consistent with a previous study showing that half of Lck-Cre/*Fbw7*$^{flox/flox}$ mice developed thymic lymphoma (3). We confirmed the accumulation of GATA3 protein at the DN stage in Lck-Cre/*Fbw7*$^{flox/flox}$ mice. Based on the expression pattern of CD2, which starts at a late DN stage, like Lck, overexpression of GATA3 must occur at this point in CD2-GATA3 Tg mice. We speculate that the induction of GATA3 in the thymus of CD2-GATA3 Tg mice and the accumulation of GATA3 in the thymus of Lck-Cre/*Fbw7*$^{flox/flox}$ mice begin at the same phase. The increased abundance of GATA3 late in the DN stage may disturb accurate progression from DN to DP and may result in transformed cells, which have been characterized as CD4$^+$ CD8$^+$ in both Lck-Cre/*Fbw7*$^{flox/flox}$ and CD2-GATA3 Tg mice (3, 37). This may imply that an appropriate amount of GATA3 is essential for the favorable development of T cells not only at the SP phase but also at an earlier phase. We indicated that depletion of Fbw7 protein in Lck-Cre/*Fbw7*$^{flox/flox}$ mice started at DN3 and was completed at DN4 and that GATA3 accumulated at DN4 in mice. We further investigated whether GATA3 accumulation at DN4 affected the proportion of DN4 subpopulations. The proportion in Lck-Cre/*Fbw7*$^{flox/flox}$ mice was not significantly different from that in *Fbw7*$^{flox/flox}$ mice (data not shown). Previous studies suggested that development from DN2 to DN3 might be affected by the deregulation of GATA3 levels. Overexpression of GATA3 in mouse fetal liver progenitors blocked the development of DN2 and DN3 cells in fetal thymus organ culture or in an OP9-DL1 coculture system (14, 38). Xu et al. (39) reported that E2A repressed GATA3 expression at the DN2 stage. In that study,

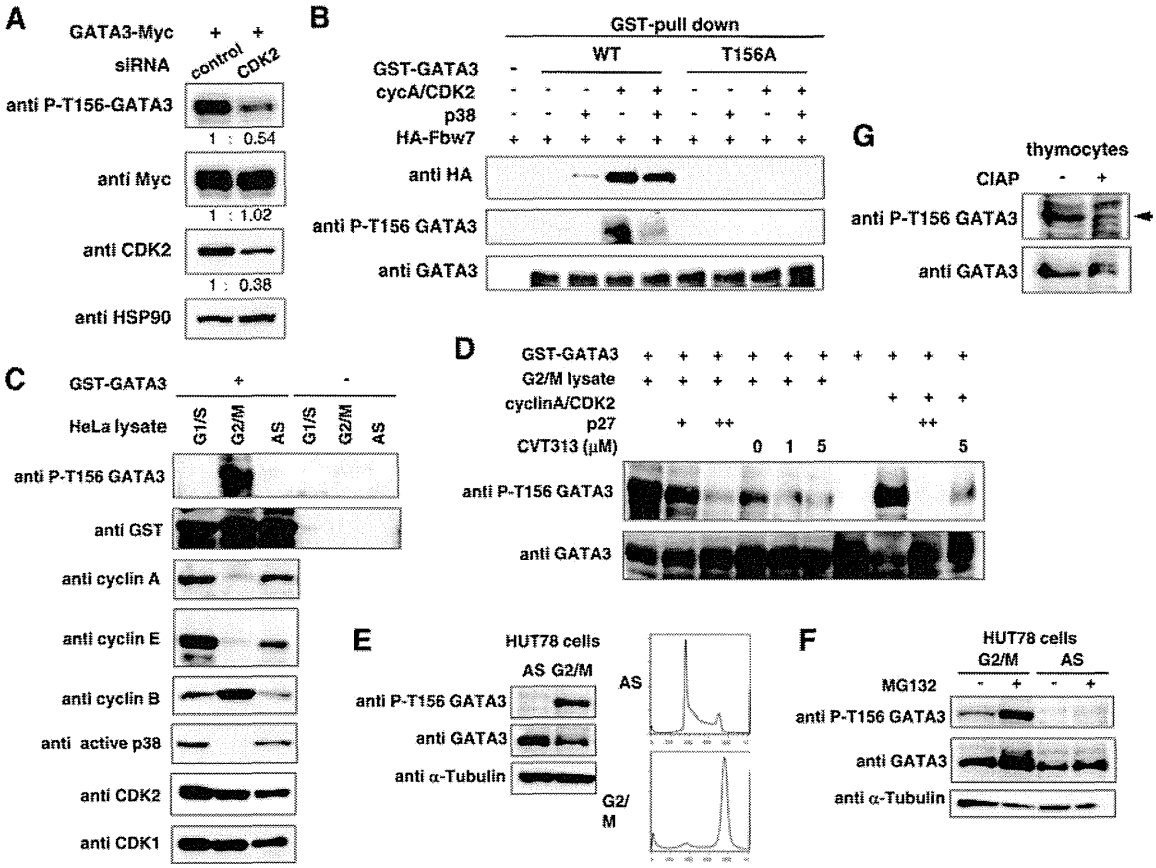

FIG 8 Phosphorylation at Thr-156 in GATA3 by CDK2 is required for association of Fbw7 and is executed in HUT78 cells during G_2/M phase and in thymocytes of mice. (A) Depletion of CDK2 reduced phosphorylation of Thr-156 in GATA3 in HEK293 cells. HEK293 cells were transfected with a WT GATA3 expression plasmid and CDK2 or a control siRNA. After 43 h of transfection, cells were treated with okadaic acid and MG132 for 5 h. Cell lysates were prepared and subjected to immunoblot analysis with the indicated antibodies. The numbers reflect the ratio of the levels of the indicated proteins between the CDK2 siRNA-transfected cells and control cells. (B) GATA3 binding to Fbw7 *in vitro* is Thr-156 phosphorylation dependent. Purified WT or T156A GST-GATA3 was incubated with the indicated kinases in reaction buffer at 30°C for 30 min. Lysates from HEK293 cells transfected with HA-Fbw7 were immunoprecipitated with HA antibody, and the immunocomplexes containing Fbw7 were incubated with phosphorylated GST-GATA3 *in vitro* as indicated. To analyze GATA3 and Fbw7 binding, the GST fusion protein complexes were precipitated using glutathione-Sepharose beads and subjected to immunoblotting with the indicated antibodies. (C and D) Phosphorylation of recombinant GATA3 *in vitro*. Reaction products were then subjected to immunoblot analysis with the indicated antibodies. (C) Phosphorylation of Thr-156 in GATA3 in G_2/M-arrested cells. GST-GATA3 was incubated with lysate prepared from either cells arrested in G_1/S or G_2/M phase or nonsynchronized (AS) HeLa cells. (D) Effects of CDK2 inhibition on Thr-156 phosphorylation of GATA3 in G_2/M cell lysate. The responsible kinase in G_2/M-phase cell lysate is CDK2. GST-GATA3 was incubated with the indicated kinase sources in the absence or presence of CDK2 inhibitor (CVT313) or competitor (p27). (E and F) Thr-156 phosphorylation of endogenous GATA3 in G_2/M phase in T-cell lymphoma HUT78 cells. G_2/M-arrested and asynchronous (AS) HUT78 cells were prepared as indicated in Materials and Methods. Cell lysates were prepared and subjected to immunoblot analysis with the indicated antibodies. (F) G_2/M-arrested and asynchronous cells were treated with or without MG132 for 5 h before harvest. Cell lysates were prepared and subjected to immunoblot analysis with the indicated antibodies. (G) Cell lysate from whole thymocytes obtained from an *Fbw7*$^{flox/flox}$ mouse at 6 weeks of age was incubated with or without calf intestinal alkaline phosphatase (CIAP) at 37°C for 30 min and subjected to immunoblot analysis with the indicated antibodies.

increased GATA3 in E2A$^{-/-}$ DN2 lineages prevented T-cell differentiation to the DN3 stage and caused an aberrant proliferation of DN2 cells. Fbw7 may be involved in development of the DN2-DN3 stage by repression of GATA3 levels. In our study using Lck-Cre/*Fbw7*$^{flox/flox}$ mice, the effects of Fbw7 depletion were focused on the DN4 stage. To evaluate the contribution of Fbw7 on GATA3 turnover in earlier DN subpopulations, Scl-Cre or Mx1-Cre driver Fbw7 knockout mice, in which depletion of Fbw7 is expected throughout the DN stages, may be useful. However, some confusion may occur when these mice are used because, in addition to GATA3, other Fbw7 targets such as Notch play roles in DN development. Data regarding GATA3-targeting genes, which are active in the DN lineage, have not been reported to date. Consequently, further observations will be required in future studies to identify phenotypes which might be obtained as a result of accumulation of GATA3 in Fbw7-depleted mice.

Aberrant expression of GATA3 was reported in classical Hodgkin lymphoma (cHL) (40). A pathological feature of cHL is the occurrence of a small number of the typical Hodgkin and Reed/Sternberg (HRS) tumor cells among a mixed cellular infiltrate. Whereas HRS cells are derived from germinal center B cells, they ectopically express GATA3. GATA3 contributes to cytokine signaling in HRS cells, which presumably has an essential role in cHL pathogenesis (40). Anomalous GATA3 expression in HRS cells is stimulated by the deregulated activity of NF-κB and Notch1, which bind directly to the GATA3 promoter (40). Intriguingly, both NF-κB and Notch1 are substrates of Fbw7 (5, 41). Therefore, once Fbw7 deficiency occurs in cHL, NF-κB and Notch1 accumu-

late and subsequently induce GATA3 expression. Further, the repressed degradation of GATA3 would enhance the malignant signal. Finally, the defect of Fbw7 in cHL may promote the development of aggressive disease caused by excess GATA3.

Although CD8 SP subsets in the thymus of the Lck-Cre/*Fbw7*$^{flox/flox}$ mice retained GATA3 expression, CD8$^+$ T cells in the spleen did not express GATA3 (Fig. 3C). The GATA3-independent pathway may be responsible for the reduced frequency of CD8$^+$ T cells in the spleen of Fbw7-deficient mice. Nonetheless, the decrease in a percentage of CD8$^+$ T cells in splenocytes of the Lck-Cre/*Fbw7*$^{flox/flox}$ mice compared with control mice was confirmed. This is consistent with results from CD2-GATA3 Tg mice showing that exogenous expression of GATA3 was not detected in splenocytes (37). We observed a significant reduction of CCR7 expression in the CD8 SP cells from Lck-Cre/*Fbw7*$^{flox/flox}$ mice compared with *Fbw7*$^{flox/flox}$ mice. Because of inadequate GATA3 levels, proper cell differentiation and exit from the thymus might be disturbed, and/or apoptosis of immature subsets might be induced in CD8 SP subsets of Lck-Cre/*Fbw7*$^{flox/flox}$ mice. Ultimately, only the normal CD8 SP subpopulation that expresses appropriate GATA3 protein levels may succeed in translocation toward peripheral organs. We detected a decrease in not only CD8$^+$ T cells but also CD4$^+$ T cells in splenocytes of the Lck-Cre/*Fbw7*$^{flox/flox}$ mice compared with control levels. A previous study showed that the CD4$^+$ T-cell subset in the spleen of CD2-GATA3 Tg mice advanced the Th2-committed phenotype although its rate was comparable to that of control mice (37). Accordingly, we speculate that some aberration, from excess GATA3 during differentiation and maturation in the thymus, persisted throughout development of CD4$^+$ T cells in the spleen. Nevertheless, similar to results in CD2-GATA3 Tg mice, in Lck-Cre/*Fbw7*$^{flox/flox}$ mice there was no significant effect on CD4 SP cells in the thymus. This might suggest that CD8 SP cells were more sensitive to changes in GATA3 than CD4 SP cells. In our experiments, GATA3 protein was markedly decreased in the CD8 SP subset after maturation of the DP lineage in control mice. In contrast, deficiency of Fbw7 resulted in accumulation of GATA3 protein in CD8 SP subsets, suggesting that Fbw7-mediated degradation plays a key role in regulating GATA3 protein levels in the subsets. Because the forced expression of GATA3 induces apoptosis and inhibits the final maturation of CD8 SP T cells, it is suggested that reduction of GATA3 is required for the satisfactory development of the CD8 SP lineage after positive selection. The proportion of CD8 SP cells in the thymic cells is dependent on the extent of apoptosis and proliferation during differentiation. It is speculated that enhanced apoptosis of CD8 SP cells in Lck-Cre/*Fbw7*$^{flox/flox}$ mice decreased their percentage in thymocytes. Consequently, GATA3 accumulation caused by the depletion of Fbw7 might induce this decrease in cell populations. However, the same explanation cannot be applied to the reduction of CD4 SP cells, because increased GATA3 was not observed to influence viability of CD4 SP cells. Indeed, it might be an effect of the accumulation of other Fbw7 substrates. Onoyama et al. also speculated that DP thymocytes had lost the ability to undergo positive selection or that the proliferation or survival of SP cells was impaired in Fbw7-deficient mice (3). Nevertheless, they suggested that the participating molecules remained to be elucidated.

In a reference database for gene expression analysis (RefExA), expression of GATA3 is observed not only in the thymus and spleen but also in salivary gland, breast, skin, bladder, kidney, placenta, and blood. RefExA also demonstrated the expression of Fbw7 in brain, breast, skin, heart, adrenal gland, intestine, stomach, and testis, in addition to thymus. Therefore, GATA3 may be regulated by Fbw7-mediated degradation in numerous tissues that express both GATA3 and Fbw7. This possibility should be investigated in the future using a tissue-specific conditional knockout system.

Many substrates of Fbw7 contain a CPD sequence, which is often phosphorylated by GSK3 (1, 4, 5, 30, 31). Although we initially predicted that the CPD in GATA3 is phosphorylated by GSK3, our data indicate that the targeting kinase is CDK2, not GSK3. Consistent with these data, we previously showed that S/T-P-X-K/R, which corresponds to the CPD sequence in GATA3, is the consensus targeting sequence of cyclin A/E-CDK2 (22). Here, we propose GATA3 as the first target of CDK2-mediated phosphorylation for degradation by Fbw7. These observations suggest that regulatory signals in addition to GSK3 participate in regulating Fbw7 substrates. Levels of these proteins, which have various functions in the development of T cells, will be maintained at the appropriate stage for proper differentiation, maturation, and survival of T cells. Because GSK3-independent phosphorylation of CPD in GATA3 is a unique Fbw7 targeting pathway, we predict that GATA3 degradation should be distinct from the other Fbw7 targets in T cells. MAPK-associated phosphorylation of GATA3 is related to the so-called emergent signals in later stages of T-cell development, while the CDK2-associated GATA3 degradation system mediated by Fbw7 may be required in early lineages for constitutive precise differentiation.

We showed that phosphorylation of Thr-156, which was an essential modification for binding of Fbw7, was mediated by CDK2. It is consistent that the phosphorylated level of intrinsic GATA3 varies during G_2/M phase in T-cell lymphoma HUT78 cells. We also detected the phosphorylation at Thr-156 of GATA3 in thymocytes of mouse. Furthermore, we clarified that Fbw7 participates in GATA3 degradation in the DN4 lineage. Because CDK2 activity is present during the G_1/S border to G_2/M stages in proliferating cells, it was speculated that CDK2-dependent phosphorylation of GATA3 and its degradation by Fbw7 in G_2/M occur in proliferating DN4 cells and T-cell lymphomas such as HUT78 cells. Our data indicated that Fbw7 also participates in GATA3 degradation in CD8 SP cells. Because cell proliferation is not present in CD8 SP cells, cell cycle-independent CDK2 activity may participate in the phosphorylation of Thr-156. Alternatively, it is possible that unknown kinases and/or other mechanisms are involved in Fbw7-mediated degradation of GATA3 in CD8 SP cells.

Finally, we propose that control of GATA3 levels by Fbw7 contributes to the fine-tuning of T-cell development.

ACKNOWLEDGMENTS

We thank M. Hakamata, M. Matsumoto, and A. Ardiyanti for technical support and N. Minegishi and T. Nakajima for useful discussions.

This work was supported in part by grants from the Ministry of Education, Culture, Sports, Science and Technology of Japan grants-in-aid 24570151 (K.K.) and 25112508 and 19057005 (M.K.).

REFERENCES

1. **Welcker M, Clurman BE.** 2008. FBW7 ubiquitin ligase: a tumour suppressor at the crossroads of cell division, growth and differentiation. Nat. Rev. Cancer **8**:83–93. http://dx.doi.org/10.1038/nrc2290.
2. **Kitagawa K, Kitagawa M.** 2012. The SCF ubiquitin ligases involved in hematopoietic lineage. Curr. Drug Targets **13**:1641–1648. http://dx.doi.org/10.2174/138945012803529974.

3. **Onoyama I, Tsunematsu R, Matsumoto A, Kimura T, de Alboran IM, Nakayama K, Nakayama KI.** 2007. Conditional inactivation of Fbxw7 impairs cell-cycle exit during T cell differentiation and results in lymphomatogenesis. J. Exp. Med. **204**:2875–2888. http://dx.doi.org/10.1084/jem.20062299.
4. **Inuzuka H, Shaik S, Onoyama I, Gao D, Tseng A, Maser RS, Zhai B, Wan L, Gutierrez A, Lau AW, Xiao Y, Christie AL, Aster J, Settleman J, Gygi SP, Kung AL, Look T, Nakayama KI, DePinho RA, Wei W.** 2011. SCF(FBW7) regulates cellular apoptosis by targeting MCL1 for ubiquitylation and destruction. Nature **471**:104–109. http://dx.doi.org/10.1038/nature09732.
5. **Fukushima H, Matsumoto A, Inuzuka H, Zhai B, Lau AW, Wan L, Gao D, Shaik S, Yuan M, Gygi SP, Jimi E, Asara JM, Nakayama K, Nakayama KI, Wei W.** 2012. SCF(Fbw7) modulates the NFκB signaling pathway by targeting NFκB2 for ubiquitination and destruction. Cell Rep. **1**:434–443. http://dx.doi.org/10.1016/j.celrep.2012.04.002.
6. **Nawijn MC, Ferreira R, Dingjan GM, Kahre O, Drabek D, Karis A, Grosveld F, Hendriks RW.** 2001. Enforced expression of GATA-3 during T cell development inhibits maturation of CD8 single-positive cells and induces thymic lymphoma in transgenic mice. J. Immunol. **167**:715–723. http://dx.doi.org/10.4049/jimmunol.167.2.715.
7. **Ellmeier W, Sawada S, Littman DR.** 1999. The regulation of CD4 and CD8 coreceptor gene expression during T cell development. Annu. Rev. Immunol. **17**:523–554. http://dx.doi.org/10.1146/annurev.immunol.17.1.523.
8. **Ting CN, Olson MC, Barton KP, Leiden JM.** 1996. Transcription factor GATA-3 is required for development of the T-cell lineage. Nature **384**:474–478. http://dx.doi.org/10.1038/384474a0.
9. **Hosoya T, Maillard I, Engel JD.** 2010. From the cradle to the grave: activities of GATA-3 throughout T-cell development and differentiation. Immunol. Rev. **238**:110–125. http://dx.doi.org/10.1111/j.1600-065X.2010.00954.x.
10. **Farrar JD, Ouyang W, Lohning M, Assenmacher M, Radbruch A, Kanagawa O, Murphy KM.** 2001. An instructive component in T helper cell type 2 (Th2) development mediated by GATA-3. J. Exp. Med. **193**:643–649. http://dx.doi.org/10.1084/jem.193.5.643.
11. **Pai SY, Truitt ML, Ho IC.** 2004. GATA-3 deficiency abrogates the development and maintenance of T helper type 2 cells. Proc. Natl. Acad. Sci. U. S. A. **101**:1993–1998. http://dx.doi.org/10.1073/pnas.0308697100.
12. **Pai SY, Truitt ML, Ting CN, Leiden JM, Glimcher LH, Ho IC.** 2003. Critical roles for transcription factor GATA-3 in thymocyte development. Immunity **19**:863–875. http://dx.doi.org/10.1016/S1074-7613(03)00328-5.
13. **Ho IC, Tai TS, Pai SY.** 2009. GATA3 and the T-cell lineage: essential functions before and after T-helper-2-cell differentiation. Nat. Rev. Immunol. **9**:125–135. http://dx.doi.org/10.1038/nri2476.
14. **Anderson MK, Hernandez-Hoyos G, Dionne CJ, Arias AM, Chen D, Rothenberg EV.** 2002. Definition of regulatory network elements for T cell development by perturbation analysis with PU.1 and GATA-3. Dev. Biol. **246**:103–121. http://dx.doi.org/10.1006/dbio.2002.0674.
15. **Hendriks RW, Nawijn MC, Engel JD, van Doorninck H, Grosveld F, Karis A.** 1999. Expression of the transcription factor GATA-3 is required for the development of the earliest T cell progenitors and correlates with stages of cellular proliferation in the thymus. Eur. J. Immunol. **29**:1912–1918. http://dx.doi.org/10.1002/(SICI)1521-4141(199906)29:06<1912::AID-IMMU1912>3.0.CO;2-D.
16. **Hernández-Hoyos G, Anderson MK, Wang C, Rothenberg EV, Alberola-Ila J.** 2003. GATA-3 expression is controlled by TCR signals and regulates CD4/CD8 differentiation. Immunity **19**:83–94. http://dx.doi.org/10.1016/S1074-7613(03)00176-6.
17. **Das J, Chen CH, Yang L, Cohn L, Ray P, Ray A.** 2001. A critical role for NF-κB in GATA3 expression and TH2 differentiation in allergic airway inflammation. Nat. Immunol. **2**:45–50. http://dx.doi.org/10.1038/83158.
18. **Amsen D, Antov A, Jankovic D, Sher A, Radtke F, Souabni A, Busslinger M, McCright B, Gridley T, Flavell RA.** 2007. Direct regulation of Gata3 expression determines the T helper differentiation potential of Notch. Immunity **27**:89–99. http://dx.doi.org/10.1016/j.immuni.2007.05.021.
19. **Fang TC, Yashiro-Ohtani Y, Del Bianco C, Knoblock DM, Blacklow SC, Pear WS.** 2007. Notch directly regulates Gata3 expression during T helper 2 cell differentiation. Immunity **27**:100–110. http://dx.doi.org/10.1016/j.immuni.2007.04.018.
20. **Yamashita M, Shinnakasu R, Asou H, Kimura M, Hasegawa A, Hashimoto K, Hatano N, Ogata M, Nakayama T.** 2005. Ras-ERK MAPK cascade regulates GATA3 stability and Th2 differentiation through ubiquitin-proteasome pathway. J. Biol. Chem. **280**:29409–29419. http://dx.doi.org/10.1074/jbc.M502333200.
21. **Nakayama K, Nagahama H, Minamishima YA, Matsumoto M, Nakamichi I, Kitagawa K, Shirane M, Tsunematsu R, Tsukiyama T, Ishida N, Kitagawa M, Hatakeyama S.** 2000. Targeted disruption of Skp2 results in accumulation of cyclin E and $p27^{Kip1}$, polyploidy and centrosome overduplication. EMBO J. **19**:2069–2081. http://dx.doi.org/10.1093/emboj/19.9.2069.
22. **Kitagawa M, Higashi H, Jung HK, Suzuki-Takahashi I, Ikeda M, Tamai K, Kato J, Segawa K, Yoshida E, Nishimura S, Taya Y.** 1996. The consensus motif for phosphorylation by cyclin D1-Cdk4 is different from that for phosphorylation by cyclin A/E-Cdk2. EMBO J. **15**:7060–7069.
23. **Hale JS, Fink PJ.** 2009. Back to the thymus: peripheral T cells come home. Immunol. Cell Biol. **87**:58–64. http://dx.doi.org/10.1038/icb.2008.87.
24. **Ehrlich LI, Oh DY, Weissman IL, Lewis RS.** 2009. Differential contribution of chemotaxis and substrate restriction to segregation of immature and mature thymocytes. Immunity **31**:986–998. http://dx.doi.org/10.1016/j.immuni.2009.09.020.
25. **Forster R, Davalos-Misslitz AC, Rot A.** 2008. CCR7 and its ligands: balancing immunity and tolerance. Nat. Rev. Immunol. **8**:362–371. http://dx.doi.org/10.1038/nri2297.
26. **Teng F, Zhou Y, Jin R, Chen Y, Pei X, Liu Y, Dong J, Wang W, Pang X, Qian X, Chen WF, Zhang Y, Ge Q.** 2011. The molecular signature underlying the thymic migration and maturation of $TCR\alpha\beta^+$ $CD4^+$ CD8 thymocytes. PLoS One **6**:e25567. http://dx.doi.org/10.1371/journal.pone.0025567.
27. **Kim JW, Ferris RL, Whiteside TL.** 2005. Chemokine C receptor 7 expression and protection of circulating $CD8^+$ T lymphocytes from apoptosis. Clin. Cancer Res. **11**:7901–7910. http://dx.doi.org/10.1158/1078-0432.CCR-05-1346.
28. **Hosoya T, Kuroha T, Moriguchi T, Cummings D, Maillard I, Lim KC, Engel JD.** 2009. GATA-3 is required for early T lineage progenitor development. J. Exp. Med. **206**:2987–3000. http://dx.doi.org/10.1084/jem.20090934.
29. **Wolfer A, Wilson A, Nemir M, MacDonald HR, Radtke F.** 2002. Inactivation of Notch1 impairs VDJβ rearrangement and allows pre-TCR-independent survival of early alpha beta lineage thymocytes. Immunity **16**:869–879. http://dx.doi.org/10.1016/S1074-7613(02)00330-8.
30. **Kitagawa K, Hiramatsu Y, Uchida C, Isobe T, Hattori T, Oda T, Shibata K, Nakamura S, Kikuchi A, Kitagawa M.** 2009. Fbw7 promotes ubiquitin-dependent degradation of c-Myb: involvement of GSK3-mediated phosphorylation of Thr-572 in mouse c-Myb. Oncogene **28**:2393–2405. http://dx.doi.org/10.1038/onc.2009.111.
31. **Busino L, Millman SE, Scotto L, Kyratsous CA, Basrur V, O'Connor O, Hoffmann A, Elenitoba-Johnson KS, Pagano M.** 2012. Fbxw7α- and GSK3-mediated degradation of p100 is a pro-survival mechanism in multiple myeloma. Nat. Cell Biol. **14**:375–385. http://dx.doi.org/10.1038/ncb2463.
32. **Cohen P, Goedert M.** 2004. GSK3 inhibitors: development and therapeutic potential. Nat. Rev. Drug Discov. **3**:479–487. http://dx.doi.org/10.1038/nrd1415.
33. **Chen CH, Zhang DH, LaPorte JM, Ray A.** 2000. Cyclic AMP activates p38 mitogen-activated protein kinase in Th2 cells: phosphorylation of GATA-3 and stimulation of Th2 cytokine gene expression. J. Immunol. **165**:5597–5605. http://dx.doi.org/10.4049/jimmunol.165.10.5597.
34. **Maneechotesuwan K, Xin Y, Ito K, Jazrawi E, Lee KY, Usmani OS, Barnes PJ, Adcock IM.** 2007. Regulation of Th2 cytokine genes by p38 MAPK-mediated phosphorylation of GATA-3. J. Immunol. **178**:2491–2498. http://dx.doi.org/10.4049/jimmunol.178.4.2491.
35. **Hinds PW.** 2003. Cdk2 dethroned as master of S phase entry. Cancer Cell **3**:305–307. http://dx.doi.org/10.1016/S1535-6108(03)00084-9.
36. **Woo RA, Poon RY.** 2003. Cyclin-dependent kinases and S phase control in mammalian cells. Cell Cycle **2**:316–324. http://dx.doi.org/10.4161/cc.2.4.468.
37. **Nawijn MC, Dingjan GM, Ferreira R, Lambrecht BN, Karis A, Grosveld F, Savelkoul H, Hendriks RW.** 2001. Enforced expression of GATA-3 in transgenic mice inhibits Th1 differentiation and induces the formation of a T1/ST2-expressing Th2-committed T cell compartment in vivo. J. Immunol. **167**:724–732. http://dx.doi.org/10.4049/jimmunol.167.2.724.
38. **Taghon T, Yui MA, Rothenberg EV.** 2007. Mast cell lineage diversion of

T lineage precursors by the essential T cell transcription factor GATA-3. Nat. Immunol. 8:845–855. http://dx.doi.org/10.1038/ni1486.

39. **Xu W, Carr T, Ramirez K, McGregor S, Sigvardsson M, Kee BL.** 2013. E2A transcription factors limit expression of Gata3 to facilitate T lymphocyte lineage commitment. Blood **121**:1534–1542. http://dx.doi.org/10.1182/blood-2012-08-449447.
40. **Stanelle J, Doring C, Hansmann ML, Kuppers R.** 2010. Mechanisms of aberrant GATA3 expression in classical Hodgkin lymphoma and its consequences for the cytokine profile of Hodgkin and Reed/Sternberg cells. Blood **116**:4202–4211. http://dx.doi.org/10.1182/blood-2010-01-265827.
41. **Hubbard EJ, Wu G, Kitajewski J, Greenwald I.** 1997. sel-10, a negative regulator of lin-12 activity in *Caenorhabditis elegans*, encodes a member of the CDC4 family of proteins. Genes Dev. **11**:3182–3193. http://dx.doi.org/10.1101/gad.11.23.3182.

Skp1-Cullin-F-box (SCF)-type ubiquitin ligase FBXW7 negatively regulates spermatogonial stem cell self-renewal

Mito Kanatsu-Shinohara[a,b,1], Ichiro Onoyama[c], Keiichi I. Nakayama[c,d], and Takashi Shinohara[a,d]

[a]Department of Molecular Genetics, Graduate School of Medicine, Kyoto University, Kyoto 606-8501, Japan; [b]Precursory Research for Embryonic Science and Technology (PRESTO) and [d]Core Research for Evolutionary Science and Technology (CREST), Japan Science and Technology Agency (JST), Tokyo 102-0076, Japan; and [c]Department of Molecular and Cellular Biology, Medical Institute of Bioregulation, Kyushu University, Fukuoka 812-8582, Japan

Edited by John J. Eppig, The Jackson Laboratory, Bar Harbor, ME, and approved May 7, 2014 (received for review January 31, 2014)

Spermatogonial stem cells (SSCs) undergo self-renewal divisions to support spermatogenesis throughout life. Although several positive regulators of SSC self-renewal have been discovered, little is known about the negative regulators. Here, we report that F-box and WD-40 domain protein 7 (FBXW7), a component of the Skp1-Cullin-F-box–type ubiquitin ligase, is a negative regulator of SSC self-renewal. FBXW7 is expressed in undifferentiated spermatogonia in a cell cycle-dependent manner. Although peptidyl-prolyl cis/trans isomerase NIMA-interacting 1 (PIN1), essential for spermatogenesis, is thought to destroy FBXW7, *Pin1* depletion decreased FBXW7 expression. Spermatogonial transplantation showed that *Fbxw7* overexpression compromised SSC activity whereas *Fbxw7* deficiency enhanced SSC colonization and caused accumulation of undifferentiated spermatogonia, suggesting that the level of FBXW7 is critical for self-renewal and differentiation. Screening of putative FBXW7 targets revealed that *Fbxw7* deficiency up-regulated myelocytomatosis oncogene (MYC) and cyclin E1 (CCNE1). Although depletion of *Myc*/*Mycn* or *Ccne1*/*Ccne2* compromised SSC activity, overexpression of *Myc*, but not *Ccne1*, increased colonization of SSCs. These results suggest that FBXW7 regulates SSC self-renewal in a negative manner by degradation of MYC.

Spermatogonial stem cells (SSCs) provide the foundation for spermatogenesis by undergoing self-renewing division (1, 2). SSCs reside in a special niche microenvironment where they are provided with self-renewal factors that stimulate proliferation. Glial cell line-derived neurotrophic factor (GDNF) is secreted from the niche to promote SSC self-renewal (3). Studies on SSCs are hampered because SSCs constitute only 0.02–0.03% of germ cells, which amounts to 2–3 $\times$ 10^4 cells per mouse testis (2, 4). Moreover, the lack of a specific marker has made it difficult to distinguish SSCs from committed spermatogonia. In 1994, a germ cell transplantation technique was developed (5), in which transplanted SSCs reinitiate spermatogenesis and produce functional sperm following microinjection into seminiferous tubules of testes. Moreover, the addition of GDNF stimulated self-renewing division of SSCs and allowed long-term expansion in vitro. Cultured cells, designated as germ-line stem (GS) cells, proliferate for at least 2 y and expand to 10^{85}-fold, creating a unique opportunity to collect a large number of SSCs for biochemical and molecular biological analyses (6).

Using these techniques, molecular regulators of SSC self-renewal have been analyzed. It is now considered that GDNF activates Harvey rat sarcoma virus oncogene (HRAS) via *Src* family kinase molecules, and cells transfected with activated HRAS underwent self-renewal division without exogenous cytokines (7). Chemical inhibition of thymoma viral proto-oncogene (AKT) or mitogen-activated protein kinase kinase 1 (MAP2K1), both of which are downstream molecules of HRAS, abrogated GS cell proliferation (8–10), suggesting that they are necessary for self-renewal division. When active *Akt* or *Map2k1* was overexpressed in GS cells, *Akt*- or *Map2k1*-transfected cells could proliferate with only fibroblast growth factor 2 (FGF2) or GDNF, respectively (8, 9). These signals up-regulate *Etv5* and *Bcl6b* (8, 11), which work in combination with other constitutively expressed transcription factors, such as zinc finger and BTB domain containing 16 (*Zbtb16*) or *Taf4b*, to drive SSC self-renewal.

Although these studies have identified several positive regulators of SSC self-renewal, little is known about the negative regulators, which would be equally important in understanding stem-cell kinetics. In this study, we analyzed the function of the F-box protein FBXW7 (also known as *Fbw7*, *Cdc4*, *Fbxw6*, or *Fbxo30*), a substrate recognition subunit of the Skp1-Cullin-F-box complex (12). FBXW7 catalyzes the ubiquitination of various molecules involved in cell-fate decision and cell-cycle regulation. We hypothesized that degradation of these critical regulators by FBXW7 influences cell-cycle regulation or fate commitment in SSCs. We tested this hypothesis by taking advantage of SSC cultures and transplantation techniques.

Results

Restricted Expression of FBXW7 in Spermatogonia. We examined FBXW7 expression in seminiferous tubules of 1-, 10-, and 42-d-old mice (Fig. S1 *A–D*). In 1-d-old testes, FBXW7 was expressed in most of the gonocytes, which are precursors of spermatogonia. However, FBXW7 expression was significantly decreased in 10-d-old mouse testes, which contain proliferating spermatogonia. All stages of germ cells are present in 42-d-old testes, but

Significance

Spermatogonial stem cells (SSCs) are at the foundation of spermatogenesis. Previous studies on SSC self-renewal have focused on the positive regulation, but we hypothesized that negative regulation of self-renewal is equally important in understanding SSC self-renewal. We show here that F-box and WD-40 domain protein 7 (FBXW7), a component of the Skp1-Cullin-F-box–type ubiquitin ligase, negatively regulates SSC self-renewal. FBXW7 is expressed only in the undifferentiated spermatogonia compartment, and its overexpression compromises SSC activity whereas *Fbxw7* deficiency enhances SSC colonization and caused accumulation of undifferentiated spermatogonia. We also demonstrate that FBXW7 regulates stability of myelocytomatosis oncogene (MYC), which increased SSC activity upon overexpression. These results suggest that FBXW7 counteracts with positive regulators of self-renewal by degrading MYC and demonstrate the importance of negative regulators of self-renewal in understanding SSC homeostasis.

Author contributions: M.K.-S. designed research; M.K.-S. and T.S. performed research; M.K.-S., I.O., and K.I.N. contributed new reagents/analytic tools; M.K.-S. and T.S. analyzed data; and M.K.-S. and T.S. wrote the paper.

The authors declare no conflict of interest.

This article is a PNAS Direct Submission.

[1]To whom correspondence should be addressed. E-mail: mshinoha@virus.kyoto-u.ac.jp.

This article contains supporting information online at www.pnas.org/lookup/suppl/doi:10.1073/pnas.1401837111/-/DCSupplemental.

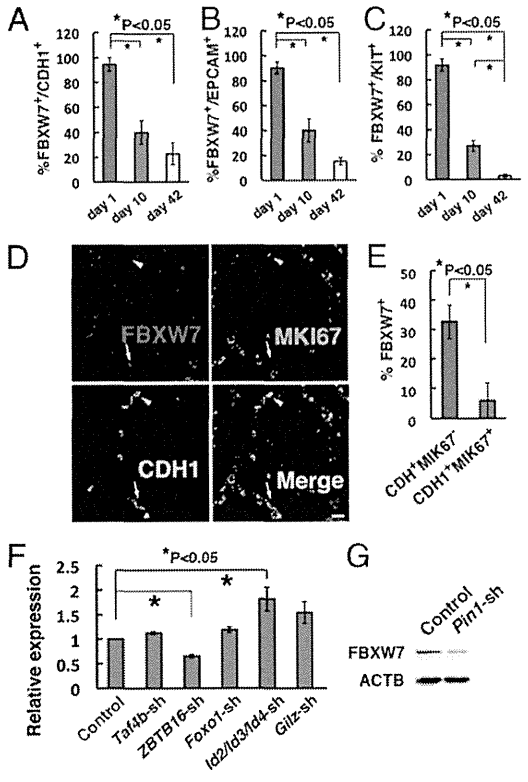

Fig. 1. Expression of FBXW7 in spermatogonia. (*A–C*) Expression of FBXW7 protein in CDH1$^+$ (*A*), EPCAM$^+$ (*B*), or KIT$^+$ (*C*) cells during postnatal testis development. At least 12, 15, and 14 tubules were counted in 1-, 10-, and 42-d-old testes, respectively. (*D*) Triple immunohistochemistry of FBXW7, MKI67, and CDH1 in 42-d-old testes. At least 17 tubules were counted. Arrows indicate CDH1$^+$MKI67$^-$ cells with FBXW7 expression. Arrowheads indicate CDH1$^+$ MKI67$^+$ cells without FBXW7 expression. (*E*) Proportion of CDH1$^+$ cells with FBXW7 expression. (*F*) Real-time PCR analysis of *Fbxw7* expression following depletion of indicated genes by shRNA ($n = 6$). (*G*) Western blot analysis of FBXW7 expression following *Pin1* depletion. (Scale bar: *D*, 20 μm.)

FBXW7 was found in only 22.7% of cadherin 1 (CDH1)-expressing undifferentiated spermatogonia and 15.1% of epitherial cell adhesion molecule (EPCAM)-expressing spermatogonia (Fig. 1 *A* and *B* and Table S1). FBXW7 was rarely found in kit oncogene (KIT)-expressing differentiating spermatogonia of adult testes (Fig. 1*C*). These results suggested that FBXW7 is expressed during the primitive stages of spermatogenesis but down-regulated during differentiation. Interestingly, FBXW7 expression was more frequently found in CDH1$^+$ antigen identified by monoclonal antibody Ki67 (MKI67)$^-$ spermatogonia compared with CDH1$^+$ MKI67$^+$spermatogonia (Fig. 1 *D* and *E*), which suggests that FBXW7 is expressed in a cell cycle-specific manner.

To examine the regulation of *Fbxw7*, we used GS cells and enriched germ cells from pup testis. Self-renewal factors, including FGF2 and GDNF, did not show an apparent effect (Fig. S2 *A* and *B*). GDNF also did not induce apparent changes in pup testis cells after gelatin selection, which are enriched for SSCs (Fig. S2 *C* and *D*). Screening of *Fbxw7* regulators using lentiviruses expressing short hairpin RNA (shRNA) revealed that depletion of *Zbtb16* reduced the expression of *Fbxw7* whereas depletion of inhibitor of DNA binding (*Id*)*2/3/4* increased *Fbxw7* mRNA expression (Fig. 1*F*, Fig. S2*E*, and Table S2). However, Western blotting showed no significant changes after these treatments (Fig. S2*F*). Nevertheless, because several F-box proteins, including FBXW7, are unstable and regulated posttranslationally (13), we also analyzed the impact of *Pin1*, a prolyl isomerase that was reported to change FBXW7 protein expression: *Pin1* overexpression down-regulated FBXW7 whereas its depletion led to elevated FBXW7 expression in human cancer cells (14). Contrary to our expectation, *Pin1* depletion down-regulated FBXW7 expression (Fig. 1*G* and Fig. S2 *E* and *G*). In contrast, *Pin1* overexpression did not influence FBXW7 expression (Fig. S2 *H* and *I*), suggesting that PIN1 is necessary but not sufficient for maintaining FBXW7 expression.

Overexpression of Fbxw7 Suppresses the Proliferation of SSCs. There are three isoforms of *Fbxw7* (*Fbxw7α*, -β, and -γ), and reverse-transcriptase (RT)-PCR analysis showed that *Fbxw7α* was strongly expressed in GS cells (Fig. 2*A*). To examine the impact of *Fbxw7α* overexpression in SSCs, lentivirus-mediated transduction of *Fbxw7α* and *Venus* was performed in testis cells from 10-d-old C57BL/6 Tg14(act-EGFP)OsbY01 (green) transgenic mice that ubiquitously express enhanced green fluorescent protein (EGFP). After overnight infection, the viral supernatant was removed, and, after 2 d, *Fbxw7α*-transduced cells were transplanted into seminiferous tubules of WBB6F1-W/W^v (W) mice. Testis cells transduced with an *Fbxw7α*-expressing vector produced 3.3 ± 0.8 colonies per 10^5 cells whereas control testis cells produced 9.2 ± 1.0 colonies per 10^5 cells ($n = 12$), and this decrease in colony number was statistically significant (Fig. 2*B* and Fig. S3*A*).

To understand the mechanism mediating the decrease in SSC induced by *Fbxw7α* overexpression, we performed transfection experiments using GS cells from B6-TgR(ROSA26)26Sor (ROSA26) mice. Flow cytometry analysis showed that *Fbxw7α* overexpression conferred a selective disadvantage for GS cell proliferation (Fig. 2 *C* and *D*). Although the proportion of cells displaying Venus fluorescence was comparable 4 d after infection, it dropped significantly after 15 d. Consistent with this observation, cell recovery was also decreased by *Fbxw7α* transfection, which suggested that *Fbxw7α* overexpression suppresses GS cell proliferation (Fig. 2*E*). This growth suppression occurred despite decreased expression of several cyclin-dependent kinase inhibitors (CDKIs) (Fig. S3*B*). Adding GDNF did not influence colonization levels of primary pup testis cells (Fig. S3*C*). Taken together, these results suggest that *Fbxw7α* overexpression has a negative impact on SSC self-renewal.

Conditional Deletion of Fbxw7 Impairs Spermatogenesis. To examine the impact of *Fbxw7* deletion on spermatogenesis, we crossed mice homozygous for the floxed *Fbxw7* allele (*Fbxw7*$^{f/f}$) with stimulated by retinoic acid gene 8 (*Stra8*)-*Cre* transgenic mice, which express *Cre* recombinase under the *Stra8*-promoter (15).

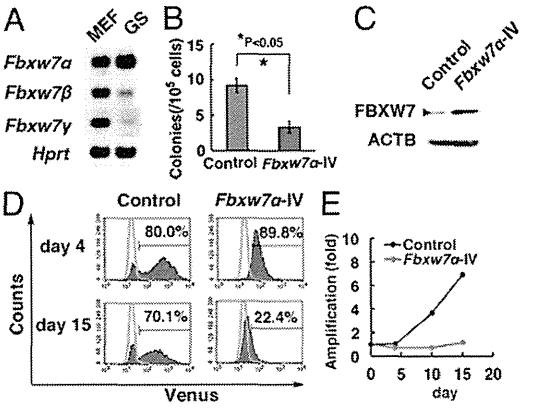

Fig. 2. Decreased SSC activity with *Fbxw7* overexpression. (*A*) RT-PCR analysis of *Fbxw7* isoform expression in GS cells and mouse embryonic fibroblasts (MEFs). (*B*) Colony counts after *Fbxw7α* overexpression and transplantation of green mouse testis cells. Results of two experiments ($n = 12$). (*C*) Western blot analysis of *Fbxw7α* expression in GS cells transduced with *Fbxw7α*. Cells were recovered 4 d after transfection. (*D*) Flow cytometric analysis of GS cells transduced with *Fbxw7α*. Cells were analyzed at the indicated time points. Green lines indicate GS cells without transfection. (*E*) Proliferation of GS cells following *Fbxw7α* overexpression.

Stra8 is a retinoic acid-responsive gene, which is first expressed a few days after birth in the majority of ZBTB16$^+$ undifferentiated spermatogonia. Testes of *Fbxw7*$^{f/f}$ *Stra8-Cre* adult mice were apparently smaller than those of controls (*Fbxw7*$^{+/+}$ *Stra8-Cre*) (Fig. 3*A*). Histological analysis of 2-mo-old *Fbxw7*$^{f/f}$ *Stra8-Cre* testes revealed significantly reduced germ cells in mutant testes, and few meiotic cells were found (Fig. 3*B*). The number of tubules with spermatogenesis, as defined by the tubules with multiple layers of germ cells, was significantly decreased by *Fbxw7* deficiency (Fig. 3*C*).

Double immunohistochemistry of the testes showed that the frequency of FBXW7-expressing cells in CDH1$^+$ spermatogonia was reduced from 20.1% in the control to 3.2% in *Fbxw7*$^{f/f}$ *Stra8-Cre* mice, suggesting that the deletion efficiency was 84.1% (Fig. 3*D* and Fig. S4*A*). We also found that expression of synaptonemal complex protein 3 (SYCP3), a marker for meiotic germ cells, was significantly suppressed in these mice (Fig. 3*E* and Fig. S4*B*). On the other hand, the seminiferous tubules of *Fbxw7*$^{f/f}$ *Stra8-Cre* mice contained a high number of CDH1$^+$ spermatogonia per Sertoli cells, as evaluated by the ratio of CDH1$^+$ to GATA binding protein 4 (GATA4)$^+$ Sertoli cells (Fig. 3*F* and Fig. S4*C*). Similar results are found for KIT (Fig. 3*G* and Fig. S4*D*), suggesting that FBXW7 plays a role in restricting the proliferation of spermatogonia. Terminal deoxynucleotidyl transferase dUTP nick end labeling (TUNEL) staining showed increased apoptosis in EPCAM$^+$ cells, but not in KIT$^+$ cells (Fig. 3 *H–J* and Fig. S4 *E* and *F*). Because EPCAM is expressed on spermatogonia and KIT is expressed on germ cells up to the pachytene stage, this observation suggests that spermatogonia are predominantly undergoing apoptosis. We also observed a greater frequency of MKI67$^+$ cells in both CDH1- and KIT-expressing spermatogonia in *Fbxw7*$^{f/f}$ *Stra8-Cre* mice (Fig. 3 *K* and *L* and Fig. S4 *G* and *H*). These results suggest that, in *Fbxw7*$^{f/f}$ *Stra8-Cre* mice, *Fbxw7* deletion not only induces the proliferation of CDH1- and KIT-expressing spermatogonia but also causes increased apoptosis of premeiotic germ cells.

Enhanced SSC Activity of Fbxw7-Deficient Testis Cells. To examine whether *Fbxw7* deficiency has any effect on SSCs, we performed transplantation experiments because SSCs cannot be identified by morphological analysis. *Fbxw7* conditional knockout (KO) mice were crossed with a ROSA26 reporter mouse strain (R26R) to visualize the pattern of colonization (16). Testis cells were collected from 8- to 11-d-old *Fbxw7*$^{f/f}$ mice heterozygous for the R26R allele, and a single-cell suspension was exposed to a *Cre*-expressing adenovirus (AxCANCre) overnight in vitro and then injected into the seminiferous tubules of W mice (Fig. 4*A* and Fig. S5*A*).

After an overnight incubation, 87.7 ± 7.1% (n = 4) and 84.3 ± 6.9% (n = 6) of the infected cells were recovered from control and mutant testis cells, respectively, showing no significant difference. Southern blot analyses showed that 63.6 ± 2.0% (n = 4) of the floxed allele was deleted at the time of transplantation (Fig. S5*B*). Analysis of the recipient testes between 6 and 8 wk showed that the testis cells from *Cre*-treated *Fbxw7*$^{f/f}$ mice produced significantly more colonies than did control testis cells (6.1 ± 1.7 and 15.3 ± 3.2 colonies per 10^5 cells injected for control and *Fbxw7*$^{f/f}$ mice, respectively; n = 18) (Fig. 4 *B* and *C*). Histological analyses showed that all of the 282 colonized tubules counted contained only a single layer of LacZ$^+$ cells on the basement membrane, and no apparent meiotic cells were found (Fig. 4*B*). Tumor formation was not observed in any of the recipient testes 6 mo after transplantation (n = 8). RT-PCR analysis of recipient testes showed

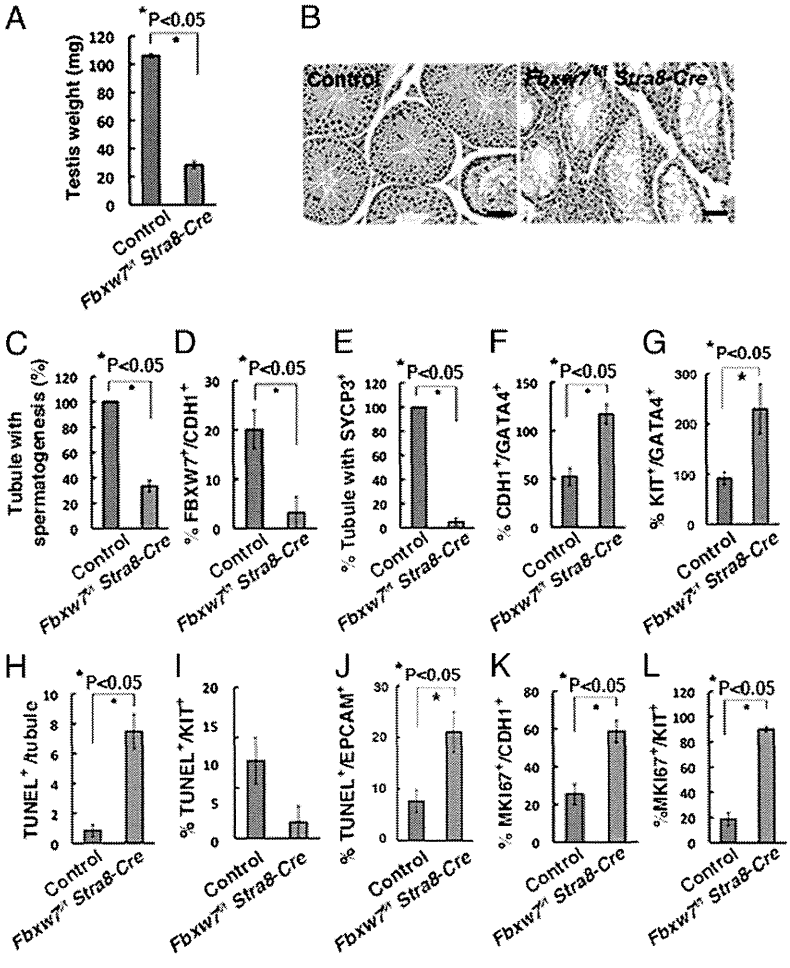

Fig. 3. Impaired spermatogenesis in *Fbxw7*$^{f/f}$ *Stra8-Cre* mice. (*A*) Testis weight of 2-mo-old *Fbxw7*$^{f/f}$ *Stra8-Cre* mice (n = 8, control; n = 6, *Fbxw7*$^{f/f}$ *Stra8-Cre*). (*B*) Histological appearance of *Fbxw7*$^{f/f}$ *Stra8-Cre* testis. (*C*) Tubules with spermatogenesis, defined as the presence of multiple layers of germ cells in the entire circumference of the tubules. At least 207 tubules were counted. (*D*) Expression of FBXW7 in CDH1$^+$ cells. At least 20 tubules were counted. (*E*) Expression of SYCP3 in KIT$^+$ cells. At least 22 tubules were counted. (*F*) Ratio of CDH1$^+$ spermatogonia and GATA4$^+$ Sertoli cells. At least 34 tubules were counted. (*G*) Ratio of KIT$^+$ spermatogonia and GATA4$^+$ Sertoli cells. At least 8 tubules were counted. (*H*) The number of TUNEL$^+$ cells in seminiferous tubules. At least 11 tubules were counted. (*I*) The number of KIT$^+$ cells undergoing apoptosis. At least 8 tubules were counted. (*J*) The number of EPCAM$^+$ cells undergoing apoptosis. At least 10 tubules were counted. (*K*) Expression of MKI67 in CDH1$^+$ cells. Eighteen tubules were counted. (*L*) Expression of MKI67 protein in KIT$^+$ cells. Twenty tubules were counted. (Scale bar: *B*, 50 μm.) Stain, hematoxylin/eosin (*B*).

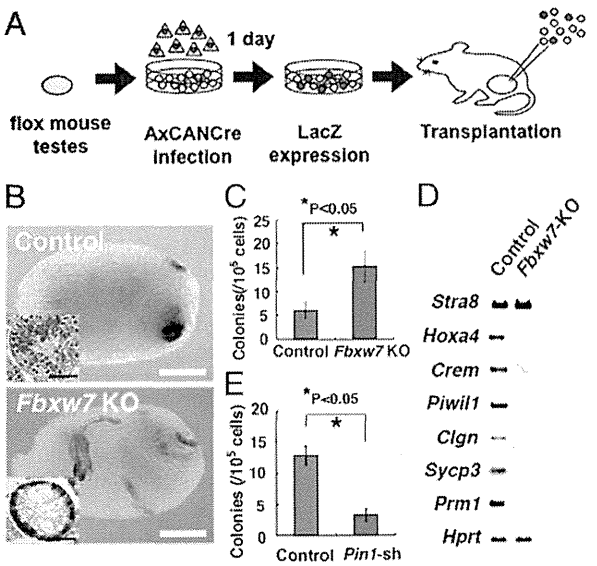

Fig. 4. Enhanced SSC activity in *Fbxw7* KO testis cells. (*A*) Experimental procedure. Testis cells from *Fbxw7*$^{f/f}$ mice were dissociated and incubated with AxCANCre overnight and then injected into the seminiferous tubules of W testes. (*B*) Macroscopic appearance of recipient testis. Histological appearance (*Inset*). (*C*) Colony counts after *Cre* transfection and transplantation of *Fbxw7*$^{f/f}$ mouse testes. Results of three experiments (n = 18). (*D*) RT-PCR analysis of spermatogenic gene expression in recipient testes. (*E*) Colony counts after *Pin1* depletion and transplantation of green mouse testes. Results of two experiments (n = 16). (Scale bars: *B*, 1 mm; *B*, *Inset*, 50 μm.)

that expression of meiotic germ cell markers, such as *Hoxa4* and *Sycp3*, was significantly reduced or not detected (Fig. 4*D*).

Although *Fbxw7* deficiency increased the concentration of SSCs, this result appeared to contradict a previous observation that *Pin1* deficiency induced spermatogonia depletion (17), given that *Pin1* depletion caused a decrease in FBXW7 level. Because PIN1 is also expressed in Sertoli cells and may influence spermatogenesis, we directly examined the impact of *Pin1* depletion in germ cells by spermatogonial transplantation. We transduced testis cells from 9-d-old green mouse pups with shRNA against *Pin1*, and the cells were transplanted into W mice 2 d later. Analysis of the recipient mice showed significantly reduced colonies with *Pin1* depletion (Fig. 4*E*). The number of colonies generated by cells transduced with control and *Pin1* shRNA was 12.9 ± 1.5 and 3.3 ± 1.0 per 10^5 cells (n = 16). This result suggests that PIN1 expression in germ cells is essential for SSC activity and that PIN1 has additional targets involved in self-renewal.

Screening of Fbxw7 Target Proteins Using GS Cells. To investigate the molecular machinery involved in FBXW7-mediated self-renewal regulation, *Fbxw7*$^{f/f}$ GS cells were established and exposed in vitro to AxCANCre overnight. Unlike the deletion of primary testis cells, Southern blot analyses showed that the floxed allele was completely deleted from the *Fbxw7* gene locus, which likely reflected enhanced proliferation of the *Fbxw7* KO population (Fig. S6*A*). Consistent with this observation, the amplification rate was increased significantly after *Cre*-mediated deletion of *Fbxw7* gene (Fig. 5*A*), which was supported by the increased frequency of MKI67$^+$ cells in mutant cells (Fig. 5*B* and Fig. S6*B*). Flow cytometric analysis showed no significant changes in the expression of known spermatogonia markers (Fig. S6*C*).

To investigate molecules involved in enhanced spermatogonial proliferation, we first examined the expression of molecules involved in cell proliferation using *Fbxw7* KO GS cells (Fig. S6*D*). We found not only increased expression of CCND1, phosphorylated MAPK14 (p-MAPK14), and AKT (p-AKT), but also decreased expression of cyclin-dependent kinase inhibitor 2B (CDKN2B) (Fig. 5*C*). We then analyzed the expression of candidate substrates of FBXW7. The expression of neither NOTCH1 nor NOTCH2 was enhanced by *Fbxw7* deficiency (Fig. S6*E*). Levels of NICD (Notch intracellular domain) did not show significant changes (Fig. S6*F*). Moreover, adding a γ-secretase inhibitor *N*-[*N*-(3,5-difluorophenacetyl)-L-alanyl]-S-phenylglycine t-butyl ester (DAPT) or depletion of *Rbpj*, the common DNA binding partner of all Notch receptors, by shRNA did not influence proliferation of *Fbxw7* KO GS cells (Fig. S6 *G*–*I*). We also checked several NOTCH target genes by real-time PCR. Although *Hes1* expression was slightly increased, the rest of the genes did not change significantly by *Fbxw7* deficiency (Fig. S6*J*). In contrast, expression of myelocytomatosis oncogene (MYC) and cyclin E1 (CCNE1) was enhanced in *Fbxw7* KO GS cells (Fig. 5*D* and Fig. S6*K*). The expression levels of phosphorylated JUN (p-JUN), v-myc myelocytomatosis viral related oncogene, neuroblastoma derived (MYCN), SREBF1, MCL1, and KLF5 did not change significantly (Fig. 5*D* and Fig. S6*K*). We also did not detect changes in MTOR level, which reportedly influenced the expression of GDNF receptor components (18). These results suggest that MYC and CCNE1 are responsible for enhanced self-renewal of SSCs.

Myc Is Responsible for Enhanced SSC Activity by Fbxw7 Deficiency. Consistent with these observations, double immunohistochemistry revealed significantly enhanced expression of MYC and CCNE1 in CDH1$^+$ undifferentiated spermatogonia in *Fbxw7*$^{f/f}$ *Stra8-Cre* mice (Fig. 5 *E* and *F* and Fig. S7 *A* and *B*). When we examined several *Myc* classic target genes, we noted increased CDK4 expression in *Fbxw7*$^{f/f}$ *Stra8-Cre* mice (Fig. 5*G* and Fig. S7 *C*–*E*). To examine whether the accumulation of MYC and/or CCNE1 caused enhanced colonization after *Fbxw7* deletion, we investigated the effect of *Myc*/*Mycn* knockdown (KD) using *Fbxw7* KO mice. We used *Mycn* and *Ccne2* shRNA because loss of *Myc* or *Ccne1* may be compensated by these treatments (19, 20). Testis cells from 7-d-old *Fbxw7*$^{f/f}$ R26R mice were transduced with lentivirus expressing shRNA for *Myc*/*Mycn* or *Ccne1*/*Ccne2* by overnight incubation, followed by treatment with AxCANCre 2 d after lentiviral infection. After overnight incubation with AxCANCre, cells were injected into W testes (Fig. 5*H*). Colonization was significantly suppressed by either *Myc*/*Mycn* or *Ccne1*/*Ccne2* KD (Fig. 5*I* and Fig. S7*F*), suggesting positive roles for these molecules in SSC self-renewal.

Finally, we examined the impact of target gene overexpression. Testis cells from 8-d-old green mice were transduced with a lentivirus expressing *Myc*, *Mycn*, or *Ccne1*. After overnight infection, the viral supernatant was removed, and the cells were transplanted into seminiferous tubules of W mice the following day. Analysis of the recipient mice showed enhanced colonization of donor cells transduced with *Myc* or *Mycn*. In contrast, *Ccne1* overexpression did not affect colonization (Fig. 5*J* and Fig. S7*G*). *Myc* overexpression could also increase colonization of pup testis transduced with *Fbxw7* (Fig. S7*H*). Although *Pin1* depletion did not change MYC in GS cells, it significantly enhanced CCNE1 (Fig. S7 *I* and *J*). *Myc* silencing in *Pin1*-depleted cells did not induce significant changes in SSC activity (Fig. S7*K*). Because *Pin1* depletion decreased SSC activity (Fig. 4*E*), these results suggest that MYC mediates the enhanced SSC activity seen with *Fbxw7* deficiency.

Discussion

Recent studies revealed that *Fbxw7* plays pivotal roles in the regulation of several stem cells/progenitors (21–25). Most of the phenotypes of *Fbxw7* deficiency are related to cell proliferation, death, or skewed differentiation. However, effects on stem cell self-renewal are not always evident and can be variable. In testes, FBXW7 expression is restricted to a subset of spermatogonia in a cell cycle-specific manner. *Fbxw7* mRNA expression was down-regulated by *Zbtb16* depletion whereas it was up-regulated by *Id2*/*Id3*/*Id4* depletion. Increased *Fbxw7* expression by *Id2*/*Id3*/*Id4* depletion was intriguing. Given that ID proteins often influence cell-cycle progression (26), it is possible that ID proteins may

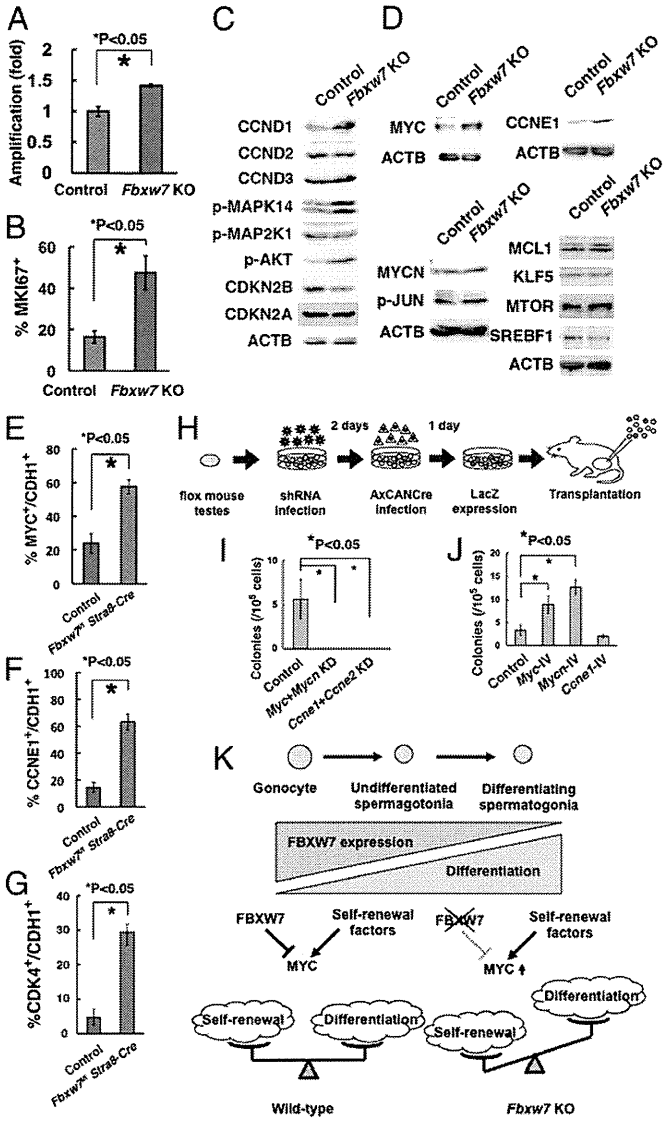

Fig. 5. Characterization of *Fbxw7* KO GS cells for target identification. (*A*) Enhanced proliferation of GS cells after *Cre* transfection. After overnight incubation with AxCANCre, virus supernatant was removed, and cells were replated in a new dish. Cell number was determined 3 d after replating. AxCANLacZ was used as a control (n = 4). Results of two experiments. (*B*) Quantification of GS cells expressing MKI67. At least 732 cells in four different fields were counted. (*C*) Western blot analysis of molecules involved in proliferation of GS cells. (*D*) Western blot analysis of FBXW7 substrates. (*E*) Expression of MYC in CDH1$^+$ cells in *Fbxw7*$^{f/f}$ *Stra8-Cre* testes. Fifteen tubules were counted. (*F*) Expression of CCNE1 in CDH1$^+$ cells in *Fbxw7*$^{f/f}$ *Stra8-Cre* testes. Fifteen tubules were counted. (*G*) Expression of CDK4 in CDH1 cells in *Fbxw7*$^{f/f}$ *Stra8-Cre* testes. At least 8 tubules were counted. (*H*) Experimental procedure. Immature testis cells from *Fbxw7*$^{f/f}$ mice were infected with lentiviruses expressing shRNA against *Myc/Mycn* or *Ccne1/Ccne2*. Culture medium was changed on the next day after infection. Two days after shRNA infection, cells were infected with AxCANCre and transplanted 24 h after AxCANCre infection. (*I*) Colony counts after depleting the indicated genes (n = 8). Results of two experiments. (*J*) Colony counts after overexpression of indicated genes and transplantation of green mouse testis cells. Results of two experiments (n = 12). (*K*) Summary of experiments. Loss of FBXW7 increases self-renewal by up-regulation of MYC and suppresses differentiation.

play a role in regulating FBXW7 expression, which occurred in a cell cycle-dependent manner. However, depletion of these molecules did not lead to apparent changes in Western blots. Our screening further revealed that FBXW7 down-regulation occurs upon depletion of *Pin1*, whose deficiency causes male infertility (17). This result was unexpected because PIN1 is thought to promote FBXW7 degradation by causing self-ubiquitination (14). Although *Pin1* overexpression did not change FBXW7 expression, it is possible that the amount of PIN1 overexpression was not sufficient to influence FBXW7. Alternatively, PIN1 may collaborate with other molecules. Because promotion of FBXW7 degradation by PIN1 was demonstrated in cancer cells, the interaction between FBXW7 and PIN1 may be more complex in nontransformed spermatogonia and may involve additional molecules. *Fbxw7* is a tumor suppressor, and its expression needs to be tightly controlled in nontransformed cells. Indeed, PIN1 expression is inversely correlated with FBXW7 expression (14) whereas PIN1 expression was enhanced in undifferentiated relative to differentiating spermatogonia (17), suggesting another sophisticated regulation system. Because *Pin1* depletion compromised SSC activity, we speculate that the balance between PIN1 and FBXW7 is critical in determining SSC fate and that disruption of this regulation may induce tumor formation. Our results suggest that PIN1 functions in a context-dependent manner to regulate FBXW7 expression.

We found that overexpression of *Fbxw7α* compromised SSC activity of testis cells. Although SSC number increased dramatically in pup testes (27), donor-cell colonization was significantly decreased by *Fbxw7α* overexpression. Given the strong growth suppression of GS cells by *Fbxw7α* overexpression and its cell cycle-specific expression, this result suggests that the amount and timing of FBXW7 need to be tightly controlled to promote cell-cycle progression. It also suggests that committed progenitors proliferate faster than undifferentiated spermatogonia because they lack FBXW7 expression. However, we currently cannot explain why *Fbxw7α* overexpression reduced the colonization activity of SSCs. It might be related to the fact that FBXW7 is restricted to undifferentiated spermatogonia in the spermatogenic system. One possibility is that *Fbxw7α* -overexpressing SSCs may have seeded in the recipient testes but ectopic *Fbxw7α* overexpression in progenitors may have hindered colony formation. It is also possible that SSCs may have failed to colonize the recipient tubules due to cell-cycle dysregulation, which is one of the important factors involved in migration of SSCs to niches (28).

Our results showed that *Fbxw7* deletion increased proliferation of undifferentiated spermatogonia. Importantly, transplantation experiments confirmed its effect on SSCs. Together with the results from *Fbxw7* overexpression experiments, these results demonstrate that FBXW7 plays an important role in negatively regulating self-renewal. To our knowledge, this is the first report of increased SSC activity in KO mice. Although enhanced spermatogonial proliferation was observed in *Cdkn1b* KO mice (29), *Cdkn1b* is different from *Fbxw7* in that its deficiency promoted differentiating division and a decreased rather than increased SSC frequency. *Tsc22d3* deficiency was also associated with increased spermatogonia proliferation, but undifferentiated spermatogonia were lost in the adult (30). Mutations in other genes, such as *Sohlh1/Sohlh2*, suppressed differentiation (31), but *Fbxw7* is unique because its deficiency not only caused enhanced proliferation of undifferentiated spermatogonia but also increased self-renewal division. In this regard, it should be noted here that enhancement of self-renewal activity was accompanied by impaired differentiation and increased apoptosis. Although *Fbxw7* deficiency often caused apoptosis and skewed differentiation, complete suppression of differentiation has not been observed in other self-renewing tissues. In this sense, the spermatogenic system appears to be extremely sensitive to the amount of FBXW7 in differentiation.

In our search for candidate FBXW7 target molecules, we found up-regulation of MYC and CCNE1 in *Fbxw7* KO GS cells. *Myc* plays a key role in exit from and reentry into the cell cycle, and its overexpression was also implicated in human tumorigenesis (32). The function of *Mycn* in spermatogonia was reported in a previous study (33), which showed that *Mycn* is up-regulated by GDNF in a phosphatidylinositol 3-kinase-AKT dependent manner to contribute to proliferation. However, because this study was carried out in an SV40-transformed spermatogonia

cell line, the role of *Myc* family genes in SSCs has remained unclear. The importance of *Ccne1* in spermatogonia was demonstrated in several studies. *Ccne1* overexpression increased SSC self-renewal by cooperating with *Ccnd2* (7) whereas *Ccne2* deficiency compromised spermatogenesis (19).

Several lines of evidence suggest that MYC is a target substrate of FBXW7 in SSCs and that it increases SSC activity. First, loss of *Fbxw7* induced accumulation of MYC in undifferentiated spermatogonia and GS cells. Second, suppression of *Myc/Mycn* by shRNAs abolished the up-regulated SSC activity caused by *Fbxw7* deficiency. Third, *Myc* or *Mycn* overexpression increased the colonization efficiency of wild-type (WT) testis cells. Although depletion of *Ccne1* and *Ccne2* expression could reduce SSC activity, *Ccne1* overexpression did not enhance colonization, suggesting that CCNE1/CCNE2 are not involved in the abnormal phenotype of *Fbxw7* KO mice. Enhanced apoptosis in *Fbxw7*-deficient testis may also be caused by increased MYC expression (32). Taken together, these lines of evidence strongly suggest that FBXW7 counteracts with positive regulators of self-renewal by degrading MYC (Fig. 5*K*).

Although the current study identified a role for FBXW7 as a negative regulator of SSC self-renewal, several questions persist. For example, although PIN1 is thought to bind to FBXW7 in a phosphorylation-dependent manner, we need to find targets for PIN1 and whether they have any interaction with FBXW7. We also do not know why FBXW7 influenced the expression of MYC, but not MYCN, and whether MYC up-regulation is involved in the suppression of spermatogonial differentiation. Having identified, to our knowledge, the first negative regulator of SSCs, we are now at the stage to find other negative regulators that may counteract with self-renewal signals at different levels. In addition, modulation of FBXW7 function by small molecules may be useful for enhancement of SSC self-renewal in vitro for genetic modifications. Thus, identification of the negative regulator for SSC self-renewal not only deepens our knowledge of SSC biology but also adds a new dimension of investigation and possibilities.

Materials and Methods

Animals. The generation of *Fbxw7*$^{f/f}$ mice was described previously (34). WT C57BL/6 mice were purchased from Japan SLC. We also used 8- to 10-d-old green mice that ubiquitously express EGFP (a gift from D. M. Okabe, Osaka University, Osaka). Male *Fbxw7*$^{f/f}$ mice were crossed with R26R female mice (16) to introduce the *LacZ* reporter construct for *Cre*-mediated deletion (The Jackson Laboratory). *Stra8-Cre* transgenic mice were also purchased from The Jackson Laboratory. Genotypes of the mice were examined by PCR with the primers listed in Table S3.

Transplantation. For transplantation, testis cells were dissociated into single-cell suspensions by a two-step enzymatic digestion using collagenase type IV and trypsin (Sigma), as described previously (35). GS cells were incubated with 0.25% trypsin to obtain single-cell suspensions. The donor cells were transplanted into seminiferous tubules of W mice (Japan SLC) through the efferent duct. Approximately 4 μL could be introduced into each testis, which filled 75–85% of the seminiferous tubules.

The Institutional Animal Care and Use Committee of Kyoto University approved all animal experimentation protocols. Further details of procedures are described in the *SI Materials and Methods*.

ACKNOWLEDGMENTS. We thank Ms. Y. Ogata for technical assistance. This research was supported by the government of Japan through its "Funding Program for Next Generation World-Leading Researchers," the Japan Science and Technology Agency (Core Research for Evolutionary Science and Technology, Precursory Research for Embryonic Science and Technology), the Mochida Memorial Foundation for Medical and Pharmaceutical Research, the Takeda Science Foundation, the Uehara Memorial Foundation, and the Ministry of Education, Culture, Sports, Science, and Technology, Japan.

1. de Rooij DG, Russell LD (2000) All you wanted to know about spermatogonia but were afraid to ask. *J Androl* 21(6):776–798.
2. Meistrich ML, van Beek MEAB (1993) Cell and molecular biology of the testis. *Spermatogonial Stem Cells*, eds Desjardins C, Ewing LL (Oxford Univ Press, New York), pp 266–295.
3. Meng X, et al. (2000) Regulation of cell fate decision of undifferentiated spermatogonia by GDNF. *Science* 287(5457):1489–1493.
4. Tegelenbosch RAJ, de Rooij DG (1993) A quantitative study of spermatogonial multiplication and stem cell renewal in the C3H/101 F1 hybrid mouse. *Mutat Res* 290(2):193–200.
5. Brinster RL, Zimmermann JW (1994) Spermatogenesis following male germ-cell transplantation. *Proc Natl Acad Sci USA* 91(24):11298–11302.
6. Kanatsu-Shinohara M, et al. (2003) Long-term proliferation in culture and germline transmission of mouse male germline stem cells. *Biol Reprod* 69(2):612–616.
7. Lee J, et al. (2009) Genetic reconstruction of mouse spermatogonial stem cell self-renewal in vitro by Ras-cyclin D2 activation. *Cell Stem Cell* 5(1):76–86.
8. Ishii K, Kanatsu-Shinohara M, Toyokuni S, Shinohara T (2012) FGF2 mediates mouse spermatogonial stem cell self-renewal via upregulation of Etv5 and Bcl6b through MAP2K1 activation. *Development* 139(10):1734–1743.
9. Lee J, et al. (2007) Akt mediates self-renewal division of mouse spermatogonial stem cells. *Development* 134(10):1853–1859.
10. Oatley JM, Avarbock MR, Brinster RL (2007) Glial cell line-derived neurotrophic factor regulation of genes essential for self-renewal of mouse spermatogonial stem cells is dependent on Src family kinase signaling. *J Biol Chem* 282(35):25842–25851.
11. Oatley JM, Avarbock MR, Telaranta AI, Fearon DT, Brinster RL (2006) Identifying genes important for spermatogonial stem cell self-renewal and survival. *Proc Natl Acad Sci USA* 103(25):9524–9529.
12. Welcker M, Clurman BE (2008) FBW7 ubiquitin ligase: A tumour suppressor at the crossroads of cell division, growth and differentiation. *Nat Rev Cancer* 8(2):83–93.
13. Pashkova N, et al. (2010) WD40 repeat propellers define a ubiquitin-binding domain that regulates turnover of F box proteins. *Mol Cell* 40(3):433–443.
14. Min S-H, et al. (2012) Negative regulation of the stability and tumor suppressor function of Fbw7 by the Pin1 prolyl isomerase. *Mol Cell* 46(6):771–783.
15. Sadate-Ngatchou PI, Payne CJ, Dearth AT, Braun RE (2008) Cre recombinase activity specific to postnatal, premeiotic male germ cells in transgenic mice. *Genesis* 46(12): 738–742.
16. Soriano P (1999) Generalized lacZ expression with the ROSA26 Cre reporter strain. *Nat Genet* 21(1):70–71.
17. Atchison FW, Means AR (2003) Spermatogonial depletion in adult Pin1-deficient mice. *Biol Reprod* 69(6):1989–1997.
18. Hobbs RM, Seandel M, Falciatori I, Rafii S, Pandolfi PP (2010) Plzf regulates germline progenitor self-renewal by opposing mTORC1. *Cell* 142(3):468–479.
19. Geng Y, et al. (2003) Cyclin E ablation in the mouse. *Cell* 114(4):431–443.
20. Laurenti E, et al. (2008) Hematopoietic stem cell function and survival depend on c-Myc and N-Myc activity. *Cell Stem Cell* 3(6):611–624.
21. Babaei-Jadidi R, et al. (2011) FBXW7 influences murine intestinal homeostasis and cancer, targeting Notch, Jun, and DEK for degradation. *J Exp Med* 208(2):295–312.
22. Hoeck JD, et al. (2010) Fbw7 controls neural stem cell differentiation and progenitor apoptosis via Notch and c-Jun. *Nat Neurosci* 13(11):1365–1372.
23. Matsumoto A, et al. (2011) Fbxw7-dependent degradation of Notch is required for control of "stemness" and neuronal-glial differentiation in neural stem cells. *J Biol Chem* 286(15):13754–13764.
24. Matsuoka S, et al. (2008) Fbxw7 acts as a critical fail-safe against premature loss of hematopoietic stem cells and development of T-ALL. *Genes Dev* 22(8):986–991.
25. Sancho R, et al. (2010) F-box and WD repeat domain-containing 7 regulates intestinal cell lineage commitment and is a haploinsufficient tumor suppressor. *Gastroenterology* 139(3):929–941.
26. Ruzinova MB, Benezra R (2003) Id proteins in development, cell cycle and cancer. *Trends Cell Biol* 13(8):410–418.
27. Shinohara T, Orwig KE, Avarbock MR, Brinster RL (2001) Remodeling of the postnatal mouse testis is accompanied by dramatic changes in stem cell number and niche accessibility. *Proc Natl Acad Sci USA* 98(11):6186–6191.
28. Ishii K, Kanatsu-Shinohara M, Shinohara T (2014) Cell-cycle-dependent colonization of mouse spermatogonial stem cells after transplantation into seminiferous tubules. *J Reprod Dev* 60(1):37–46.
29. Kanatsu-Shinohara M, Takashima S, Shinohara T (2010) Transmission distortion by loss of p21 or p27 cyclin-dependent kinase inhibitors following competitive spermatogonial transplantation. *Proc Natl Acad Sci USA* 107(14):6210–6215.
30. Bruscoli S, et al. (2012) Long glucocorticoid-induced leucine zipper (L-GILZ) protein interacts with ras protein pathway and contributes to spermatogenesis control. *J Biol Chem* 287(2):1242–1251.
31. Suzuki H, et al. (2012) SOHLH1 and SOHLH2 coordinate spermatogonial differentiation. *Dev Biol* 361(2):301–312.
32. Eilers M, Eisenman RN (2008) Myc's broad reach. *Genes Dev* 22(20):2755–2766.
33. Braydich-Stolle L, Kostereva N, Dym M, Hofmann M-C (2007) Role of Src family kinases and N-Myc in spermatogonial stem cell proliferation. *Dev Biol* 304(1):34–45.
34. Onoyama I, et al. (2007) Conditional inactivation of Fbxw7 impairs cell-cycle exit during T cell differentiation and results in lymphomatogenesis. *J Exp Med* 204(12): 2875–2888.
35. Ogawa T, Aréchaga JM, Avarbock MR, Brinster RL (1997) Transplantation of testis germinal cells into mouse seminiferous tubules. *Int J Dev Biol* 41(1):111–122.

Supporting Information

Kanatsu-Shinohara et al. 10.1073/pnas.1401837111

SI Materials and Methods

Cell Culture. Germ-line stem (GS) cells used in the present study were derived from green mice or ROSA26 mice that were backcrossed to a DBA/2 background (1, 2). We derived *Fbxw7*$^{f/f}$ GS cells from 2- to 3-d-old *Fbxw7*$^{f/f}$ mice produced from offspring that resulted from crossing *Fbxw7*$^{f/+}$ mice in a C57BL/6 × DBA/2 background. GS cell culture conditions using StemPro-34 SFM (Invitrogen) were described previously (1). The growth factors used included 10 ng/mL human fibroblast growth factor 2 (FGF2), and 15 ng/mL rat glial cell line-derived neurotrophic factor (GDNF) (Peprotech). The cells were regularly maintained on mitomycin C (Sigma)-treated mouse embryonic fibroblasts (MEFs). *N*-[*N*-(3,5-difluorophenacetyl)-L-alanyl]-*S*-phenylglycine t-butyl ester (DAPT) (Wako Pure Chemical Industries) was added at 10 μM.

Immunostaining. Testes samples were fixed in 4% paraformaldehyde for 2 h and then frozen in Tissue-Tek OCT compound (Sakura Finetechnical). For immunostaining of cryosections, samples were treated with 0.1% Triton X-100 in PBS. After immersing them in blocking buffer (0.1% Tween 20, 3% BSA, and 10% goat serum in PBS) for >1 h, samples were incubated with primary antibodies at 4 °C overnight. Secondary antibodies were incubated for 1 h at room temperature. Samples were counterstained with Hoechst 33342 (Sigma). The images were collected using a confocal microscope (Fluoview FV1000D; Olympus). The antibodies used are listed in Table S1.

Flow Cytometry. GS cells were dissociated by incubating in cell dissociation buffer for 5 min (Invitrogen). Propidium iodide (1 μg/mL) was added to exclude dead cells. Stained cells were analyzed using a FACSCalibur (BD Biosciences). The antibodies used are listed in Table S1.

Lentivirus Infection. Full-length mouse *Fbxw7α*, human *Myc* (a gift from H. Saya, Keio University, Tokyo), human *Mycn* (Addgene), and human *Ccne1* (a gift from C. J. Sherr, St. Jude Children's Research Hospital, Memphis, TN) were cloned into the CSII-EF-IRES2-Venus (IV) vector. Human *Pin1* (Addgene) was cloned into the CSII-EF-IRES2-puro (IP) vector. Lentiviral particles were produced by transient transfection of 293T cells, and GS cells or testis cells were transfected as described previously (3). Virus titers were determined by transfecting 293T cells, and the multiplicities of infection (MOIs) were adjusted to 4.0.

Increases in the number of *Fbxw7α*-expressing GS cells were measured by plating 3×10^5 cells per 9.5 cm^2 on MEFs. The number of Venus-expressing cells was determined by FACSCalibur (BD Biosciences). For transplantation experiments, green mouse testis cells were transfected with the control or *Fbxw7α*-expressing lentiviral construct, and 6×10^4 cells were transplanted into seminiferous tubules 2 d after transfection.

For shRNA-mediated gene knockdown (KD), KD vectors were purchased from Open Biosystems. A mixture of lentiviral particles was used to transfect GS cells from ROSA mice or testis cells. pLKO1-Scramble shRNA (Addgene) was used as a control (Open Biosystems). The lentivirus titer was determined using a Lenti-X p24 rapid titer kit (Clontech). The MOIs in the KD experiment were adjusted to 4.0. All KD vectors are listed in Table S2.

Adenovirus Infection. For deletion of *Fbxw7*, dissociated testis cells were exposed to AxCANCre (RIKEN BRC) at a density of 1×10^6 cells per 9.5 cm^2, as described previously (4). After overnight incubation, the virus was removed on the next day, and cells were used for transplantation. AxCANLacZ (RIKEN BRC) was used as a control. The MOIs were adjusted to 2.0.

Apoptosis Assay. For TUNEL staining, a single-cell suspension was concentrated on glass slides by centrifugation with Cytospin 4 (Thermo Electron Corporation). After fixation in 4% paraformaldehyde for 1 h, cells were labeled using an In Situ Cell Death Detection kit (TMR red) (Roche Applied Science) according to the manufacturer's protocol. The nuclei were counterstained with Hoechst 33342 (2 μg/mL; Sigma) to determine the percentage of TUNEL-positive nuclei relative to the total number of Hoechst 33342-stained nuclei. Apoptotic cells were quantified by collecting images of stained cells using Photoshop software (Adobe Systems).

Analyses of Recipient Testes. For counting the colony number, recipient mice were killed between 6 and 8 wk after transplantation, and their testes were analyzed by observation under UV light or by staining for β-galactosidase, the *LacZ* gene product, with 5-bromo-4-chloro-3-indolyl-β-D-galactopyranoside (X-gal) (Wako Pure Chemical Industries) (2). In experiments using green mice, testes were analyzed under UV fluorescence. A germ-cell cluster was defined as a colony when it occupied the entire basal surface of the tubule and was longer than 0.1 mm. For histological analysis, paraffin-embedded sections were stained with hematoxylin/eosin. The number of tubules with spermatogenesis, as defined by the presence of multiple layers of germ cells in the entire circumference of the tubules, was recorded for one section from each testis.

Southern Blotting. Genomic DNA was digested with StuI and transferred and hybridized with exon 4 probe, as described previously (4, 5). The PCR product was subsequently cloned into pGEMT easy vector (Promega). The plasmid was then digested with EcoRI to produce a 322-bp fragment, which was used as a hybridization probe. Band intensity was quantified using NIH image 1.62 software.

Western Blotting. Samples were separated by SDS/PAGE, transferred onto Hybond-P membranes (Amersham Biosciences), and incubated with primary antibodies. The antibodies used in the experiments are shown in Table S1. Band intensity was quantified using Multi Gauge version 3.0 software (Fuji Photo Film Co. Ltd.), and expression levels were normalized relative to those of ACTB.

Gene-Expression Analyses. Total RNA was isolated using TRIzol (Invitrogen), and first-strand cDNA was synthesized using a Verso cDNA Synthesis Kit (Thermo Fisher Scientific) for RT-PCR. For real-time PCR, the StepOnePlus Real-Time PCR system and *Power* SYBR Green PCR Master Mix were used following the manufacturer's protocol (Applied Biosystems). Transcript levels were normalized relative to those of *Hprt*. PCR conditions were 95 °C for 10 min, followed by 40 cycles of 95 °C for 15 s, and 60 °C for 1 min. Each PCR was run at least in triplicate. For RT-PCR, PCR conditions were 95 °C for 10 min, followed by 30 cycles at 95 °C for 15 s, 60 °C for 30 s, and 72 °C for 1 min. The primers used for PCR are listed in Table S3.

Statistical analyses. Results are presented as means ± SEM. Significant differences between means for single comparisons were determined using the Student *t* test. Multiple comparison analyses were performed using ANOVA followed by Tukey's Honest Significant Difference (HSD) test.

1. Kanatsu-Shinohara M, et al. (2003) Long-term proliferation in culture and germline transmission of mouse male germline stem cells. *Biol Reprod* 69(2):612–616.
2. Kanatsu-Shinohara M, et al. (2011) Serum- and feeder-free culture of mouse germline stem cells. *Biol Reprod* 84(1):97–105.
3. Kanatsu-Shinohara M, et al. (2008) Long-term culture of male germline stem cells from hamster testes. *Biol Reprod* 78(4):611–617.
4. Takehashi M, et al. (2007) Adenovirus-mediated gene delivery into mouse spermatogonial stem cells. *Proc Natl Acad Sci USA* 104(8):2596–2601.
5. Onoyama I, et al. (2007) Conditional inactivation of Fbxw7 impairs cell-cycle exit during T cell differentiation and results in lymphomatogenesis. *J Exp Med* 204(12):2875–2888.

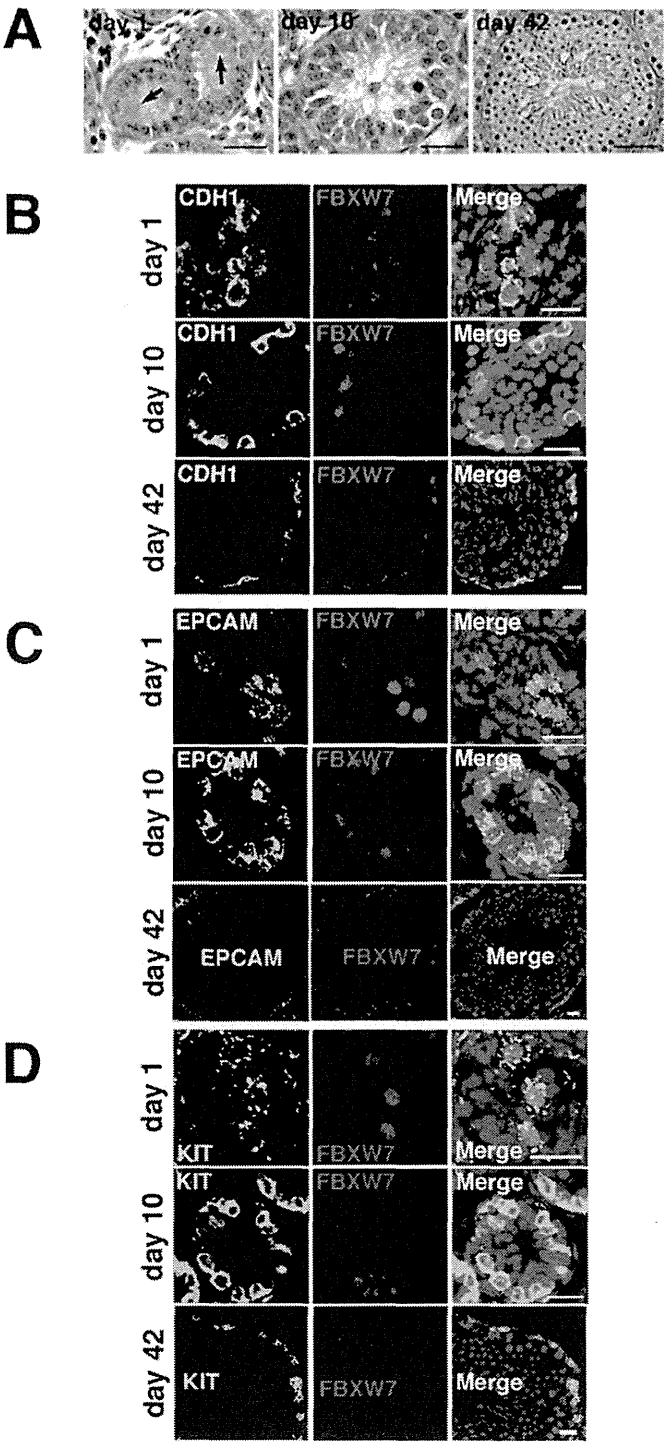

Fig. S1. Expression of F-box and WD-40 domain protein 7 (FBXW7) in testes. (*A*) Histological appearance of postnatal testes. Arrows indicate gonocytes that are not attached to the basement membrane. (*B–D*) Double immunohistochemistry of FBXW7 and cadherin 1 (CDH1) (*B*), epitherial cell adhesion molecule (EPCAM) (*C*), or kit oncogene (KIT) (*D*) during postnatal testis development. (Scale bars: *A*, 50 μm; *B–D*, 20 μm.) Stain: *A*, hematoxylin/eosin; *B–D*, Hoechst 33342.

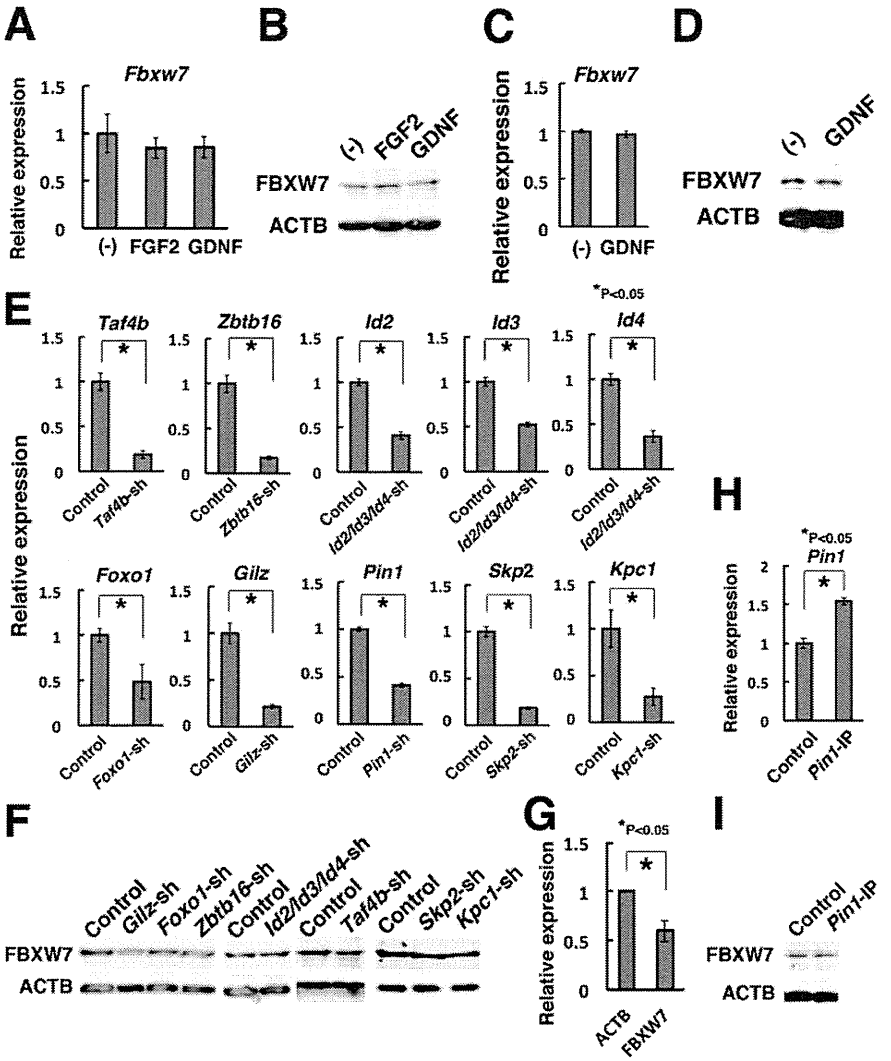

Fig. S2. Regulation of *Fbxw7* expression. (*A*) Real-time PCR analysis of *Fbxw7* expression by cytokine supplementation in GS cells. GS cells were cultured without cytokines for 3 d, and samples were collected 24 h after cytokine supplementation ($n = 9$). (*B*) Western blot analysis of FBXW7 expression by cytokine supplementation in GS cells. GS cells were cultured without cytokines for 3 d, and samples were collected 24 h after cytokine supplementation. (*C* and *D*) Expression of *Fbxw7* (*C*) and FBXW7 (*D*) in germ cells enriched from 10-d-old pup testes. Testis cells were incubated overnight on gelatin-coated plates. Germ cells were enriched by gentle pipetting and cultured on laminin-coated plates for 2 d without GDNF. Samples were collected 24 h after GDNF supplementation. Results of real-time PCR (*C*) ($n = 9$) and Western blot analysis (*D*) are shown. Increase in FBXW7 expression was 1.2 ± 0.2-fold ($n = 3$), and the difference was not significant. (*E*) Real-time PCR analysis of indicated gene expression following depletion by shRNA ($n = 6$–9). Cells were recovered 3 d after infection. (*F*). Western blot analysis of FBXW7 expression following depletion of indicated genes by shRNA. Cells were recovered 3 d after infection. (*G*) Quantification of FBXW7 expression in GS cells following *Pin1* depletion by shRNA ($n = 3$). Cells were recovered 3 d after infection. (*H*) Real-time PCR analysis of *Pin1* expression following *Pin1* overexpression in GS cells ($n = 3$). Cells were recovered 3 d after infection. (*I*) Western blot analysis of FBXW7 expression in GS cells following *Pin1* overexpression. Increase in FBXW7 expression was 1.2 ± 0.1-fold ($n = 3$), and the difference was not significant.

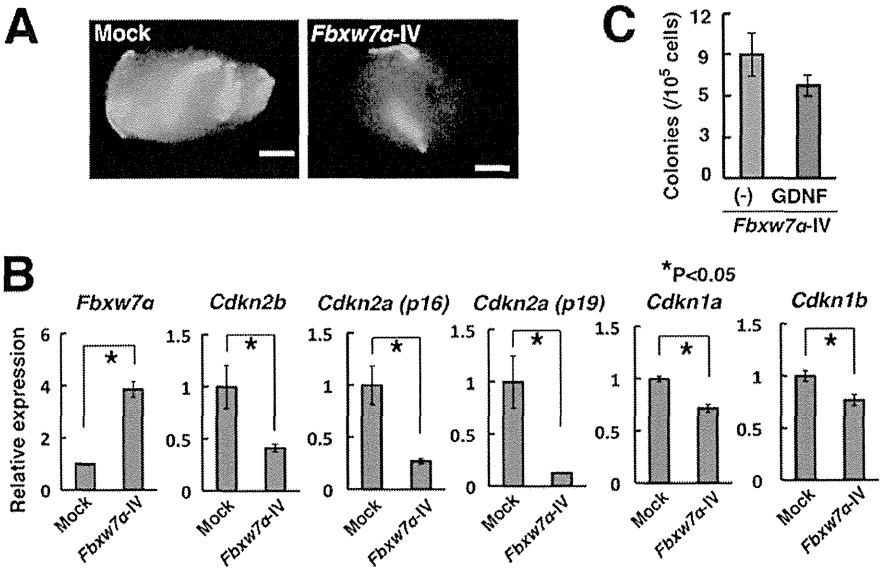

Fig. S3. Overexpression of *Fbxw7α* in GS cells. (*A*) Macroscopic appearance of a W recipient testis after transplantation of green mouse testis cells transduced with *Fbxw7α*. Cells were transplanted 2 d after infection. Colonized areas appear as green stretches of tubules under UV light. (*B*) Real-time PCR analyses of the indicated genes following *Fbxw7α* overexpression (n = 6–9). Cells were recovered 3 d after infection. (*C*) Colony counts after *Fbxw7α* overexpression and incubation with GDNF. Results of 3 experiments (n = 18). (Scale bar: *A*, 1 mm.)

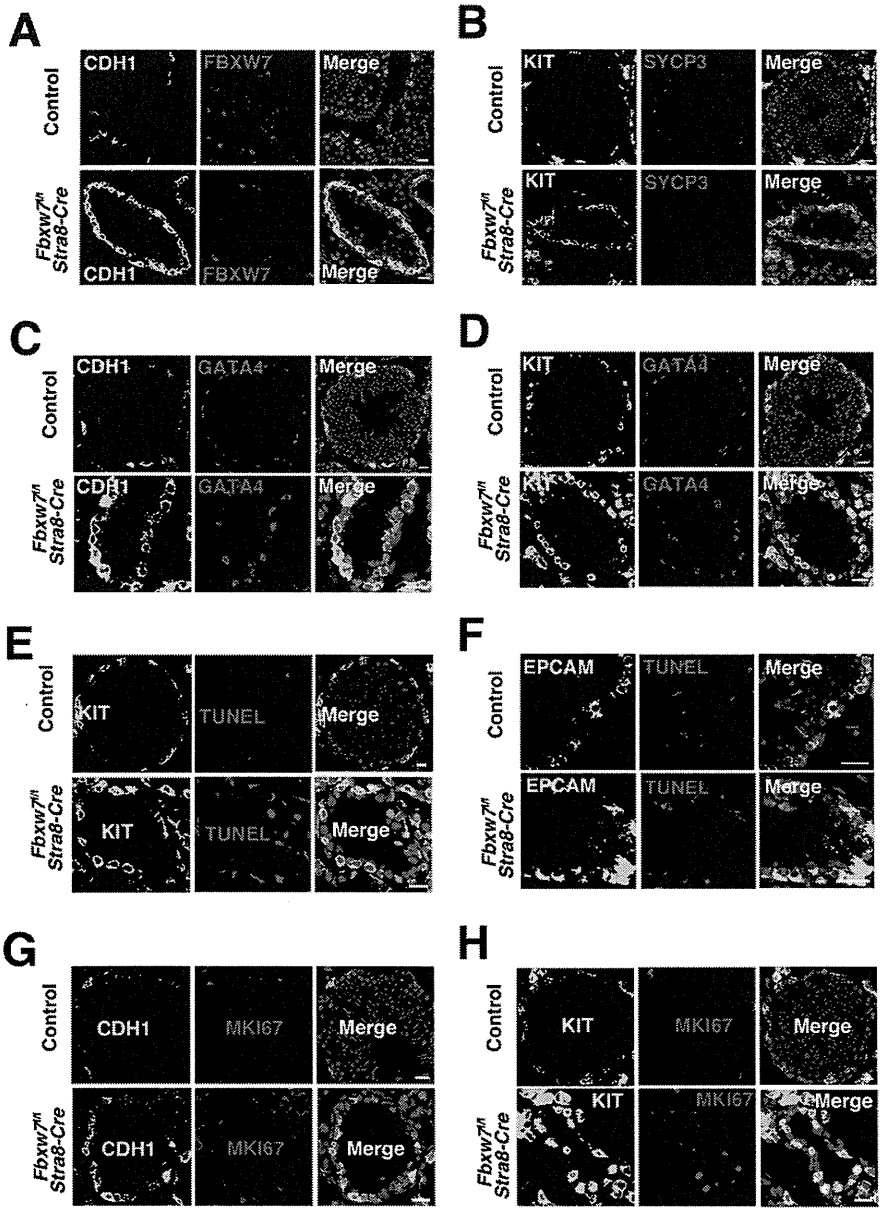

Fig. S4. Immunohistochemistry of *Fbxw7*$^{f/f}$ stimulated by retinoic acid gene 8 (*Stra8*)-*Cre* mouse testes. (*A*) Double immunohistochemistry of FBXW7 and CDH1. (*B*) Double immunohistochemistry of KIT and synaptonemal complex protein 3 (SYCP3). (*C*) Double immunohistochemisty of CDH1 and GATA binding protein 4 (GATA4). (*D*) Double immunohistochemistry KIT and GATA4. (*E*) Immunohistochemical staining of KIT and TUNEL. (*F*) Immunohistochemical staining of EPCAM and TUNEL. (*G*) Double immunohistochemistry of CDH1 and antigen identified by monoclonal antibody Ki67 (MKI67). (*H*) Double immunohistochemistry of KIT and MKI67. Counterstained with Hoechst 33342 (blue). (Scale bar: 20 μm.) Stain: *A–H*, Hoechst 33342.

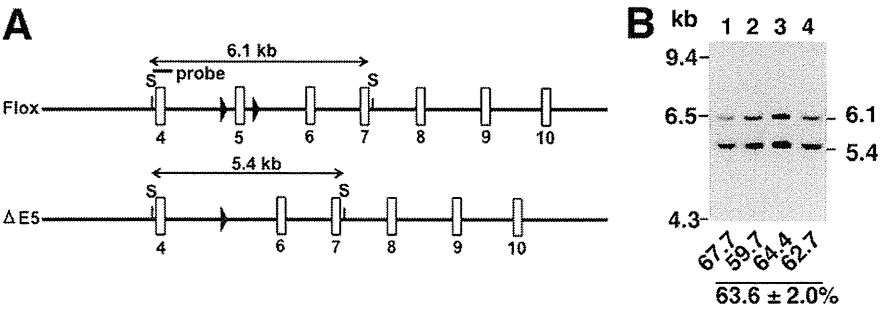

Fig. S5. Production of *Fbxw7* KO SSCs by AxCANCre transduction. (*A*) Conditional mutant mice used in the experiment. Exon 5 of the *Fbxw7* gene was deleted by Cre-mediated recombination. The indicated probe was used for Southern blot analysis. S, StuI. (*B*) Southern blot analysis to detect the deletion efficiency. Genomic DNA was digested with StuI and hybridized with the indicated probe.

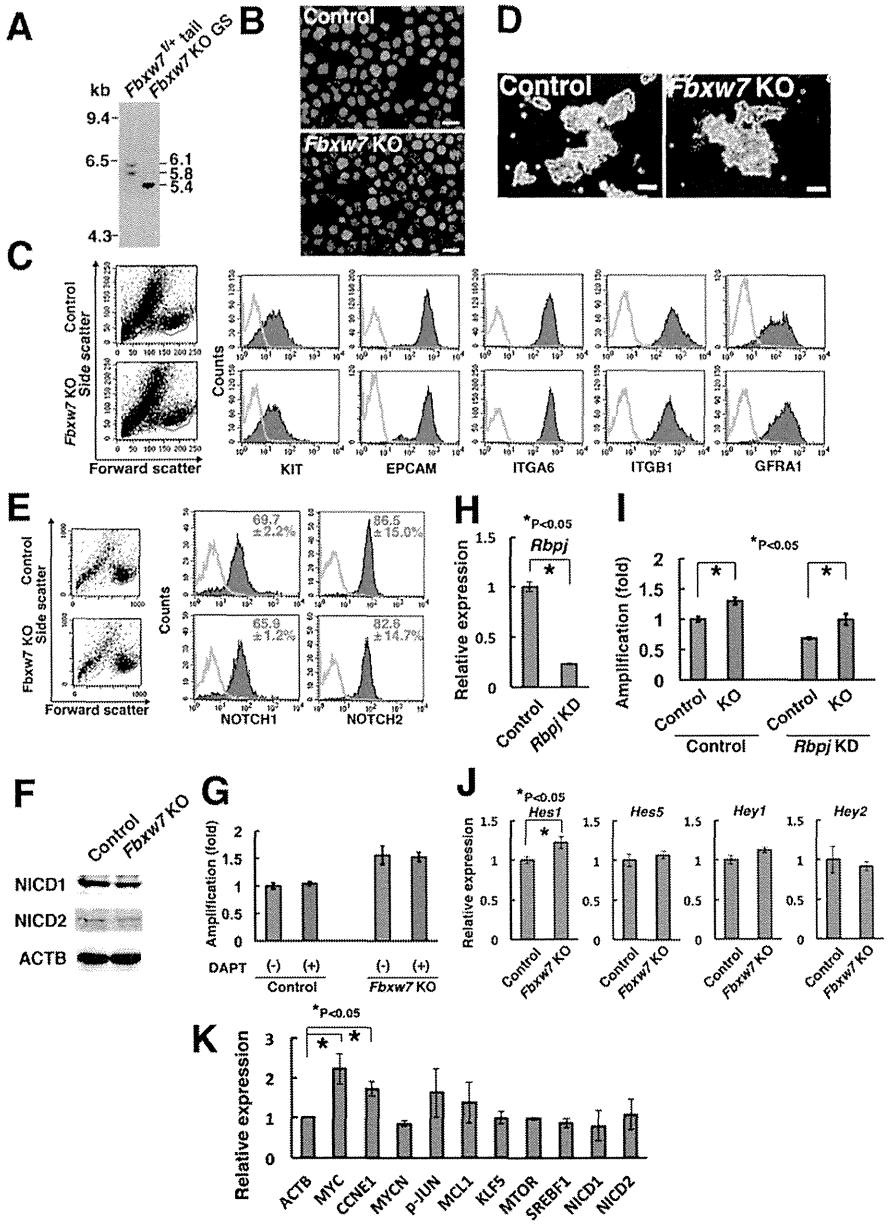

Fig. S6. Phenotype of *Fbxw7* KO GS cells. (*A*) Southern blot analysis of *Fbxw7* KO GS cells 3 wk after AxCANCre infection. (*B*) Immunocytochemistry of MKI67 in *Fbxw7* KO GS cells. Three days after infection. (C) Flow cytometric analysis of spermatogonia marker expression. Green lines indicate controls. (*D*) Appearance of *Fbxw7* knockout (KO) GS cells. (*E*) Flow-cytometric analysis of NOTCH1 and NOTCH2 expression ($n = 3$–4). (*F*) Western blot analysis of NICD1 and NICD2 expression. (*G*) Effect of DAPT on *Fbxw7* KO GS cell proliferation ($n = 6$). After overnight inoculation with AxCANCre, virus supernatant was removed, and cells were replated with DAPT after passage. Cell number was determined 3 d after replating. AxCANLacZ was used as a control. (*H*) Real-time PCR analysis of *Rbpj* expression following depletion by shRNA ($n = 9$). Cells were recovered 3 d after infection. (*I*) Effect of *Rbpj* depletion on *Fbxw7* KO GS cell proliferation ($n = 3$). *Fbxw7* KO GS cells were infected with shRNA against *Rbpj* and were replated after 24 h. The cells were then incubated with AxCANCre for 24 h. Virus supernatant was removed, and cells were replated in a new dish. Cell number was determined 3 d after replating. AxCANLacZ was used as a control. (*J*) Real-time PCR analysis of NOTCH target gene expression. ($n = 9$). (*K*) Quantification of Western blot band intensities for FBXW7 substrates ($n = 3$–4). (Scale bars: *B* and *D*, 20 μm.)

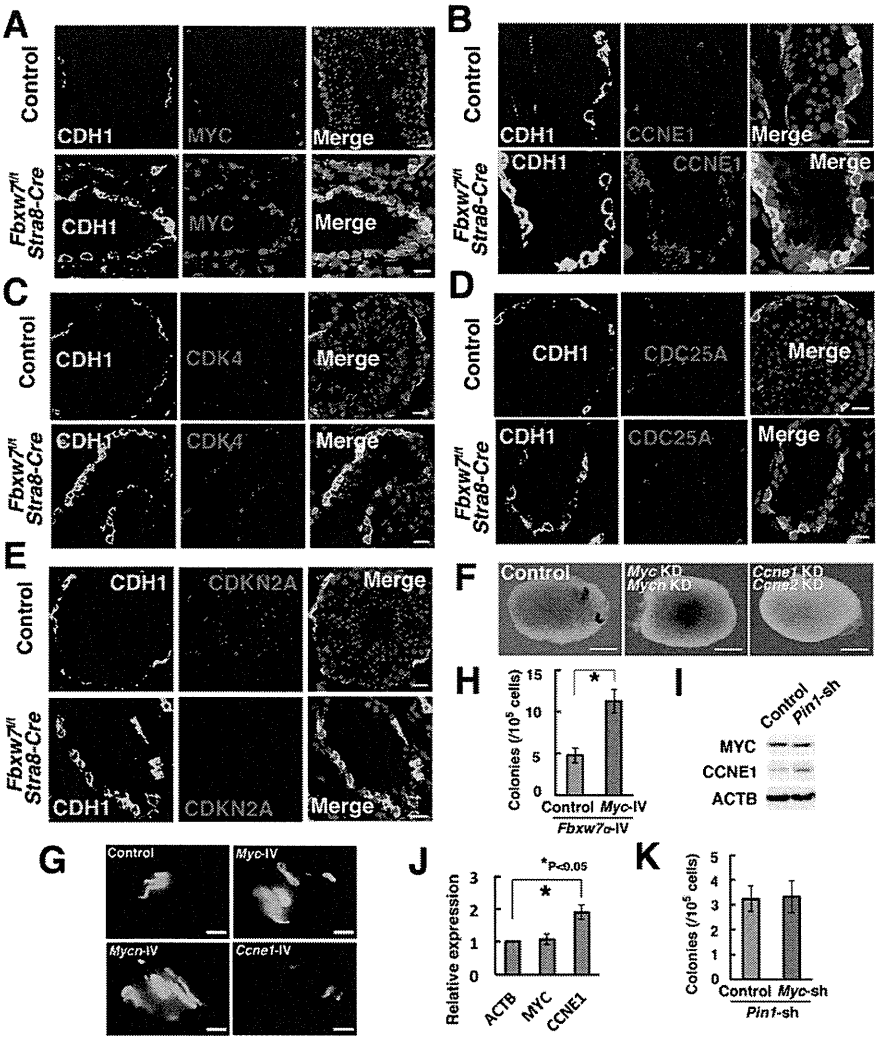

Fig. S7. Effect of Fbxw7 deficiency in myelocytomatosis oncogene (MYC) or cyclin E1 (CCNE1) expression. (*A*) Double immunohistochemistry of CDH1 and MYC in *Fbxw7*$^{f/f}$ *Stra8-Cre* testes. (*B*) Double immunohistochemistry of CDH1 and CCNE1 in *Fbxw7*$^{f/f}$ *Stra8-Cre* testes. (*C*) Double immunohistochemistry of CDH1 and CDK4 in *Fbxw7*$^{f/f}$ *Stra8-Cre* testes. (*D*) Double immunohistochemistry of CDH1 and CDC25A in *Fbxw7*$^{f/f}$ *Stra8-Cre* testes. (*E*) Double immunohistochemistry of CDH1 and cyclin-dependent kinase inhibitor (CDKN) 2A in *Fbxw7*$^{f/f}$ *Stra8-Cre* testes. (*F*) Macroscopic appearance of recipient testes transplanted with *Fbxw7* KO testis cells after transduction of shRNAs against *Myc*/*Mycn* or *Ccne1*/*Ccne2*. (*G*) Macroscopic appearance of recipient testes transplanted with green mouse testis cells transduced with a lentivirus expressing *Myc*, *Mycn*, or *Ccne1*. (*H*) Colony counts after overexpression of *Fbxw7α* and *Myc*. Results of three experiments ($n = 16$). (*I* and *J*) Effect of *Pin1* depletion by shRNA on MYC and CCNE1 expression. Western blot analysis (*I*) and quantification of band intensities (*J*) are shown ($n = 3$). Cells were recovered 3 d after infection. (*K*) Colony counts after depletion of *Pin1* and *Myc*. Results of three experiments ($n = 18$). (Scale bars: *A*–*E*, 20 μm; *F* and *G*, 1 mm.) Stain: *A*–*E*, Hoechst 33342.